To date, resistant variants to C-HR-derived peptides, such as T-20 and C34, have been extensively investigated. Resistant variants to T-20 have emerged with mutations in the N-HR region, especially from L33 to L45, which is thought to be the binding site of T-20, both *in vitro* (Fikkert et al., 2002; Rimsky et al., 1998) and *in vivo* (Aquaro et al., 2006; Bienvenu et al., 2006; Cabrera et al., 2006; Labrosse et al., 2006; Menzo et al., 2004; Perez-Alvarez et al., 2006; Ray et al., 2007; Wei et al., 2002), suggesting that substitutions in the N-HR directly interfere with T-20 binding. Variants resistant to C34 also emerged in vitro with amino acid mutations in the N-HR region (Armand-Ugon et al., 2003; Lohrengel et al., 2005; Nameki et al., 2005). Taken together, mutations in the N-HR region play a key role in resistance to C-HR-derived peptides.

An N-HR-derived peptide N36 corresponding to the leucine/isoleucine zipper sequence of gp41 has anti-HIV-1 activity to a lesser extent when compared to T-20 and C34 (Dubay et al., 1992; Wild et al., 1994; Wild et al., 1992). It is believed that N36 easily aggregates in physiological solutions, resulting in reduced potency (Lu et al., 1995; Lu and Kim, 1997). Meanwhile, a stabilized and trimeric coiled-coil N peptide, IZN17, was developed and displayed 100-fold greater potency compared with N36 (Eckert and Kim, 2001a). Moreover, $(CCIZN17)_3$, a covalently stabilized trimer of IZN17s, represented 30-fold increase in potency compared with IZN17 (Bianchi et al., 2005). These studies demonstrated that appropriate engineering of N-HR-derived peptides could increase their inhibitory effect, suggesting that development of N-HR-derived peptides is one of the novel candidates for effective HIV-1 inhibitors.

In this study, we selected for and characterized HIV-1 variants resistant to N36 by virological, biochemical and X-ray crystallographic analyses, with the aim of elucidating further information regarding HIV-1 fusion.

2. Materials and methods

2.1. Cells and viruses

MT-2 and 293T cells were grown in RPMI 1640 medium and Dulbecco's modified Eagle medium (DMEM), respectively. HeLa-CD4-LTR-β-gal cells were kindly provided by M. Emerman through the AIDS Research and Reference Reagent Program, Division of AIDS, National Institute of Allergy and Infectious Disease (Bethesda, MD, USA), and used for the drug susceptibility assay as described previously (Nameki et al., 2005). Recombinant infectious HIV-1 clones carrying various mutations were generated by pNL4-3 plasmid with site-directed mutagenesis as described previously (Nameki et al., 2005). Each molecular clone was transfected into 293T cells with *TransIT*® (Mirus Bio LLC, Madison, WI, USA). After 48 h, the supernatants were harvested and stored at −80 °C until required.

2.2. Antiviral agents

The peptides used in this study were synthesized as described previously (Otaka et al., 2002). A reverse transcriptase inhibitor, 2′,3′-dideoxycytidine (ddC), and an adsorption inhibitor, dextran sulfate (DS5000) were purchased from Sigma–Aldrich (St. Louis, MO, USA).

2.3. Determination of drug susceptibility

The peptide sensitivity of infectious clones was determined by the multinuclear activation of galactosidase indicator (MAGI) assay as described previously (Nameki et al., 2005). Briefly, the target cells (HeLa-CD4-LTR-β-gal; 10^4 cells/well) were plated in 96-well flat-bottomed microtiter culture plates. On the following day, the cells were inoculated with the HIV-1 clones (60 MAGI unit/well, giving 60 blue cells after 48 h of incubation) and cultured in the presence of various concentrations of drugs in fresh medium. Forty-eight hours after viral exposure, cells were stained with X-Gal (5-bromo-4-chloro-3-indolyl-β-D-galactopyranoside) and blue cells were counted in each well. The activity of test compounds was determined as the effective concentration that blocked HIV-1 replication by 50% (EC_{50}).

2.4. Induction of HIV-1 variants resistant to N36

MT-2 cells were exposed to wild-type HIV-1 (HIV-1_{WT}) and cultured in the presence of N36 at an initial concentration of 0.1 μM. Cultures were incubated at 37 °C until extensive cytopathic effect (CPE) was observed. The culture supernatants were used for further passage of MT-2 cells in the presence of increasing concentrations of N36 until massive CPE was seen at earlier stages of culture. Such dose-escalating culture was performed until resistant variants were obtained. This selection was carried out for a total of 25 passages. At the indicated passages, 10, 20, and 22, the sequence of the *env* region was determined by direct sequencing of the proviral DNA extracted from the infected MT-2 cells.

2.5. Viral replication kinetics assay

MT-2 cells (10^5 cells/mL) were infected with each virus preparation (500 MAGI unit) for 16 h. The infected cells were then washed and cultured in a final volume of 3 mL. The culture supernatants were collected from days 2–7 after infection, and the amount of p24 antigen was determined.

2.6. Circular dichroism (CD) spectroscopy

Each peptide was incubated at 37 °C for 30 min, with the final concentration of peptides were 10 μM in phosphate buffered saline (PBS) pH 7.4. CD spectra were recorded on a AVIV model 202 spectropolarimeter (AVIV) with a 1 mm path-length cuvette at 25 °C from an average of eight scans. The thermal stability was assessed by monitoring the change in the CD signal at 222 nm. The midpoint of the thermal unfolding transition, the melting temperature (T_m) of each complex was determined as described previously (Otaka et al., 2002).

2.7. Crystallization, data collection and refinement

Crystallization was performed using the hanging-drop vapor-diffusion method at 4 °C. The solution for crystallization was prepared by mixing 2 μL peptide solution (10 mg/mL each of N36 and $C34_{KQ}$ peptides) with 2 μL of mother liquor. The triangular prism-shaped crystals of the N36/$C34_{KQ}$ complex were grown in 80 mM ammonium chloride, 16% 2-methylpentan-2,4-diol and 25% isopropanol, which diffract to beyond 1.7 Å resolution and belong to space group *C*2 with unit-cell parameters $a = 88.63$, $b = 50.48$, $c = 56.15$ Å, $\beta = 90.88°$. X-ray diffraction data were collected at 100 K on a rotating copper-anode home X-ray source (MicroMax-007, Rigaku, Japan) equipped with an imaging plate detector (*R*-axis IV^{++}, Rigaku). The structure was solved by molecular replacement using the program MOLREP (Vagin and Teplyakov, 1997) with the model of a wild-type 6-helical bundle structure which was generated by symmetry operations from the PDB coordinate file 1AIK. Structure refinement was performed with the programs CNS (Brunger et al., 1998) and XtalView (McRee, 1999).

3. Results

3.1. Selection of N36-resistant HIV-1

In order to induce HIV-1 variants resistant to N36, escalating doses of N36 (from 0.1 μM) were applied to HIV-1_{WT}-infected MT-2 cells. At passage 11 (P-11), P-20 and P-22, when the concentration of N36 was 6.4, 12.8 and 25.6 μM, respectively, the sequence of the *env* region was determined by direct sequencing of the proviral DNA extracted from MT-2 cells as described previously (Fig. 1) (Nameki et al., 2005). Sequence analysis of HIV-1 at P-11 revealed that the aspartic acid residue at position 36 (D36) and the asparagine at position 126 (N126) of gp41 had been substituted for glycine (D36G) and lysine (N126K), respectively. At P-20 and P-22, E137Q in gp41 and P183Q in gp120 had emerged, respectively. Both N126K and E137Q substitutions were located in the C-HR which is thought to be the interactive site of N36 (Fig. 1A) (Chan et al., 1997). An N126K mutation was also induced in resistant viruses to C34 (Nameki et al., 2005), T-20 (Baldwin et al., 2004), modified C-HR-derived peptide, T-1249 (Eggink et al., 2008), and cell membrane-anchored C-peptide, maC46 (Hermann et al., 2009). In the bulk-sequencing, we found mixed substitution at N126K, AAG and AAA. Therefore, we cloned PCR products to a cloning vector pSL301 (Invitrogen, Carlsbad, CA, USA) and revealed that 6 and 3 clones were AAG and AAA, respectively, and that no other substitutions in the both HRs were observed.

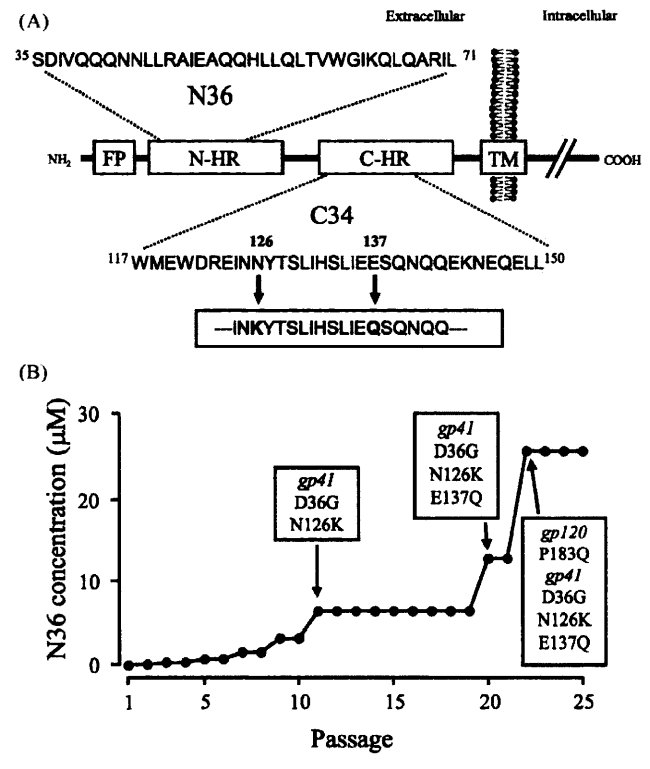

Fig. 1. Schematic view of HIV-1 gp41 (A) and induction of N36-resistant HIV-1 (B). The locations of the fusion peptide (FP), N-terminal heptad repeat region (N-HR), C-terminal heptad repeat region (C-HR), transmembrane domain (TM), and the gp41-derived peptides, N36 and C34, are shown (A). The residue numbers of each peptide correspond to their positions in gp41. The bold underlined letters in the box indicate the novel mutations that were observed in the C-HR of N36-resistant HIV-1 variants. (B) HIV-1_{WT} was passaged in MT-2 cells with increasing concentrations of N36. The dose-escalating selection was carried out for a total of 25 passages, with compound concentrations ranging from 0.1 to 25.6 μM. At the indicated passages, proviral DNA from the lysates of infected cells were sequenced.

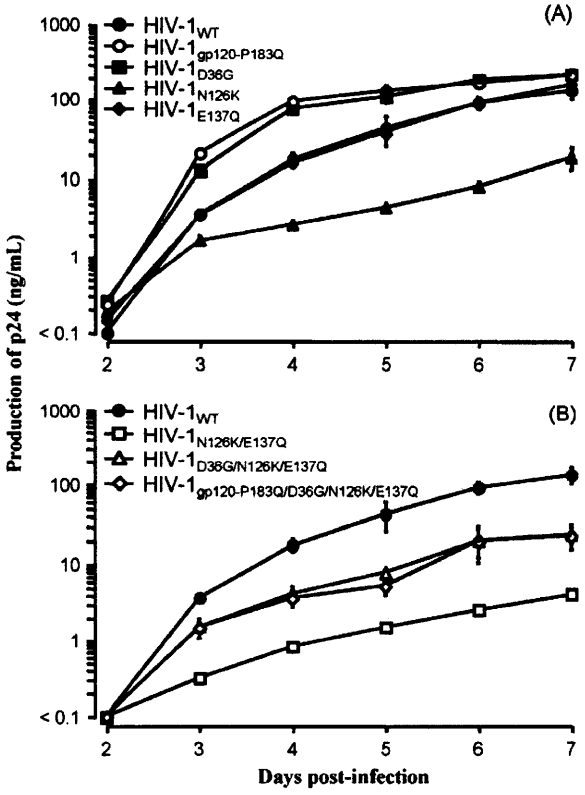

Fig. 2. Replication kinetics of N36-resistant variants. Replication kinetics of N36-resistant HIV-1 variants with a single (A) or combination of mutations (B). Supernatants were collected on days 2–7 from infected MT-2 cells and were subjected to determination of p24 production. Representative results show the mean and standard deviation of experiments performed independently three times.

3.2. Susceptibility of HIV-1 variants to N36

To identify which substitutions were responsible for N36 resistance, we generated seven recombinant viruses, and examined the susceptibility of N36 against these viruses with the MAGI assay. HIV-1_{N126K}, HIV-1_{E137Q}, HIV-$1_{N126K/E137Q}$, HIV-$1_{D36G/N126K/E137Q}$, and HIV-$1_{gp120\text{-}P183Q/D36G/N126K/E137Q}$ showed reduced susceptibility to N36 (Table 2). Since N126K emerged in HIV-1 variants resistant to C-HR-derived peptides (Baldwin et al., 2004; Nameki et al., 2005), all N126K containing viruses also demonstrated a 4–5-fold reduction in susceptibility to C34. The D36G substitution, observed in the majority of HIV-1 strains (Kuiken et al., 2009), and P183Q in gp120 demonstrated no resistance to all the inhibitors tested. P183Q which is located in the gp120 V2 region was observed in a wide range of HIV-1 subtypes including subtypes A, B, and C as well as the wild-type, indicating that P183Q is a polymorphism (Kuiken et al., 2009). These results indicate that the single mutations, N126K and E137Q, are involved in resistance to N36, but when both mutations were present, only a weak effect on resistance was observed.

3.3. Replication kinetics of N36-resistant variants

To address effects of the mutations on HIV-1 replication, we examined replication kinetics of HIV-1 variants through p24 production in culture supernatants. The N126K substitution had an adverse effect on replication kinetics, while E137Q exhibited no effect on replication kinetics compared to HIV-1_{WT} (Fig. 2A). The variant, HIV-$1_{N126K/E137Q}$ had markedly reduced replication kinetics, however the D36G mutation moderately restored these kinetics

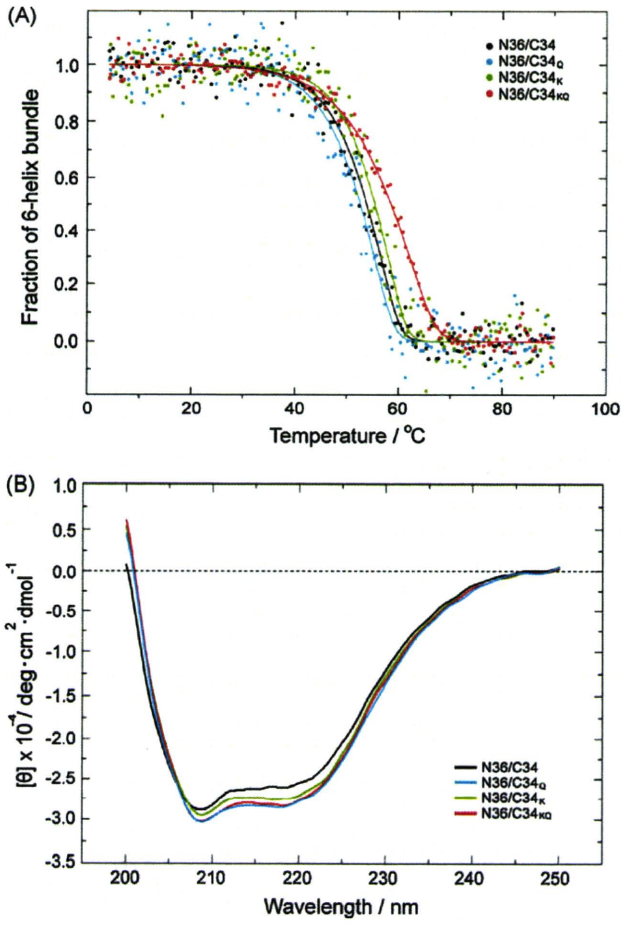

Fig. 3. Affinity of N36 and C34 with or without mutation. Melting temperature (T_m) and CD spectra of the N36/C34 (wild-type), N36/$C34_K$, N36/$C34_Q$ and N36/$C34_{KQ}$ complexes are shown (A). CD spectra profile of N36/C34 and N36/$C34_{KQ}$ complexes are shown (B).

(Fig. 2B). These results indicate that the primary mutations, N126K and E137Q, are strongly and weakly associated with a reduction in HIV-1 replication kinetics, respectively. In contrast, P183Q in gp120 solely enhanced the replication kinetics of HIV-1 (Fig. 2A) but did little to alter the replication kinetics of HIV-$1_{D36G/N126K/E137Q}$ (Fig. 2B). P183Q and D36G appear to be secondary or spontaneous mutations in HIV-1 induced by serial passage in an attempt to adapt to a cell culture environment.

3.4. Thermal stability of the 6-helix bundle

Synthetic peptides representing the N- and C-HRs have been shown to fold into thermally stable 6-helix bundles (Lu et al., 1999; Lu and Kim, 1997), and thus provide a model of gp41 for investigating structural and other biophysical properties of a 6-helix bundle. To determine whether N126K and E137Q contributed to the stability of the 6-helix bundle, we measured the T_m of the complexes, N36/C34 (wild-type) and N36/$C34_{KQ}$ (C34 with N126K and E137Q mutations). As shown in Fig. 3A, T_m values of the complex of N36/$C34_K$ and N36/$C34_Q$ were similar to that of N36/C34 complex, while that of N36/$C34_{KQ}$ was increased. In addition, the CD spectra observed in N36/$C34_{KQ}$ and N36/$C34_Q$ at 25 °C showed a high helix extent compared to that in N36/C34, while N36/$C34_K$ showed intermediate helicity (Fig. 3B). These results indicate that the two mutations, N126K and E137Q, co-operatively provide high thermal stability of the N36/$C34_{KQ}$ complex.

Table 1
Crystallization data, statistics and refinement parameters.

Crystallization	
Peptide solution	
N36	10 mg/mL
$C34_{KQ}$	10 mg/mL
Mother liquor	
Ammonium chloride	80 mM
2-Methylpentan-2,4-diol	16%
Isopropanol	25%
Data collection	
Resolution range/Å	35–1.7
No. of observed reflections	99,054
No. of unique reflections	27,434
Completeness	99.1%
Redundancy	3.61
R_{merge}	7.2%
Space group	*C*2
Unit-cell parameters	$a = 88.63, b = 50.48, c = 56.15$ Å, $\beta = 90.88°$
Refinement	
Resolution range/Å	23.8–1.7
No. of reflections in the working set	25,818
No. of protein atoms	1803
No. of water molecules	146
R/R_{free}	18.8/21.9%

3.5. Crystal structure of the 6-helix bundle

To reveal the structural basis of the resistance and stabilization mechanisms by the double mutations, we solved the crystal structure of the N36/$C34_{KQ}$ complex (PDB code 3AHA). The statistics for data collection and refinement are summarized in Table 1. The solved structure showed a 6-helix bundle structure, which was the same as in the wild-type N36/C34 complex (PDB code 1AIK) (Fig. 4). Their main chain structures are completely identical in helical pitch as well as in twist angle. A careful comparison between the N36/C34 and N36/$C34_{KQ}$ complexes revealed some differences in side-chain interactions. The N36/C34 complex has been solved in the trigonal *P*321 space group so that the asymmetric unit contains one of each N36 and C34 peptide, in which symmetrical side-chain interactions along the 3-fold rotation axis are formed around the bundle. We solved the N36/$C34_{KQ}$ complex in the lower symmetry *C*2 space group, and this asymmetric unit contained one helix bundle structure (Fig. 4).

The N126K mutation does not seem to induce conformational changes in the crystal structure when compared to the N36/C34 complex (Fig. 4C). It is consistent with the location of N126 that the N126K mutation does not directly interact with the binding groove formed by the N-HR trimer (Fig. 4A). In the case of E137Q, local rearrangement of a hydrogen bond was induced (Fig. 4D–G), although the hydrogen bond network formed by E/Q137-N43-R46-N42-Q142′-Q40′ is maintained. These asymmetrical and inter-helical side-chain interactions may contribute to the stability of gp41.

4. Discussion

In this study, we induced N36-resistant variants of HIV-1 *in vitro* and characterized them. The variants contained four mutations, P183Q in gp120 and D36G, N126K, and E137Q in gp41. Among these mutations, N126K and E137Q were directly associated with N36 resistance. The N126K mutation also conferred resistance in HIV-1 to C-HR-derived peptides (Baldwin et al., 2004; Eggink et al., 2008; Nameki et al., 2005) and a cell surface expressed peptide (Hermann et al., 2009), indicating that N126K is a key mutation for acquisition

of resistance to all gp41-derived fusion inhibitors.

E137Q was not observed as a polymorphism (Kuiken et al., 2009) and was not identified in HIV-1 that was resistant to the N-HR-derived peptide, N13ΔTrimer, which had reasonable solubility, high helicity and thermostability (Dwyer et al., 2008). Therefore, E137Q is a novel mutation for N36 resistance. The solved crystal structure revealed that E137Q induces local rearrangement of the hydrogen bond network in gp41. A polymorphism E137K (Kuiken et al., 2009) has been identified as one of resistance associated mutations to N44 in a CCR5 tropic HIV strain, HIV-$1_{JR\text{-}CSF}$ (Desmezieres et al., 2005). Recently, Tolstrup et al. (2007) also reported that E137K restored T-20-resistant virus infectivity impaired by the acquisition of the N43D mutation. Since E137 formed hydrogen bonds with N43, it is likely that the E137K mutation partially restores the 6-helix bundle stability (Bai et al., 2008), suggesting that E137 is an important position for stability of the 6-helix bundle and E137Q is a mutation for conferring N36-resistance in HIV-1. On the other hand, the overall structure of the 6-helix bundle with mutations was barely affected, which is consistent with our recent observations. The C34 derivative, SC34EK, which contains 12 hydrophilic and one artificial substitution (Nishikawa et al., 2009) has highly potent anti-HIV activity and maintains its structure in the 6-helix bundle even with these extensive modifications. These results indicate that the basic structure of the 6-helix bundle appears to be crucial for gp41 function, suggesting that agents which disrupt this structure will have inhibitory effects upon fusion.

Other substitutions observed in the N36 selection, P183Q in gp120 and D36G in gp41, enhanced viral replication kinetics (Fig. 2) but little influenced N36 susceptibility (Table 2). It is likely that faster entry kinetics theoretically provides resistance to fusion inhibitors through relatively short period to allow interaction of fusion inhibitors with the target, gp41. Indeed, HIV-1 with the

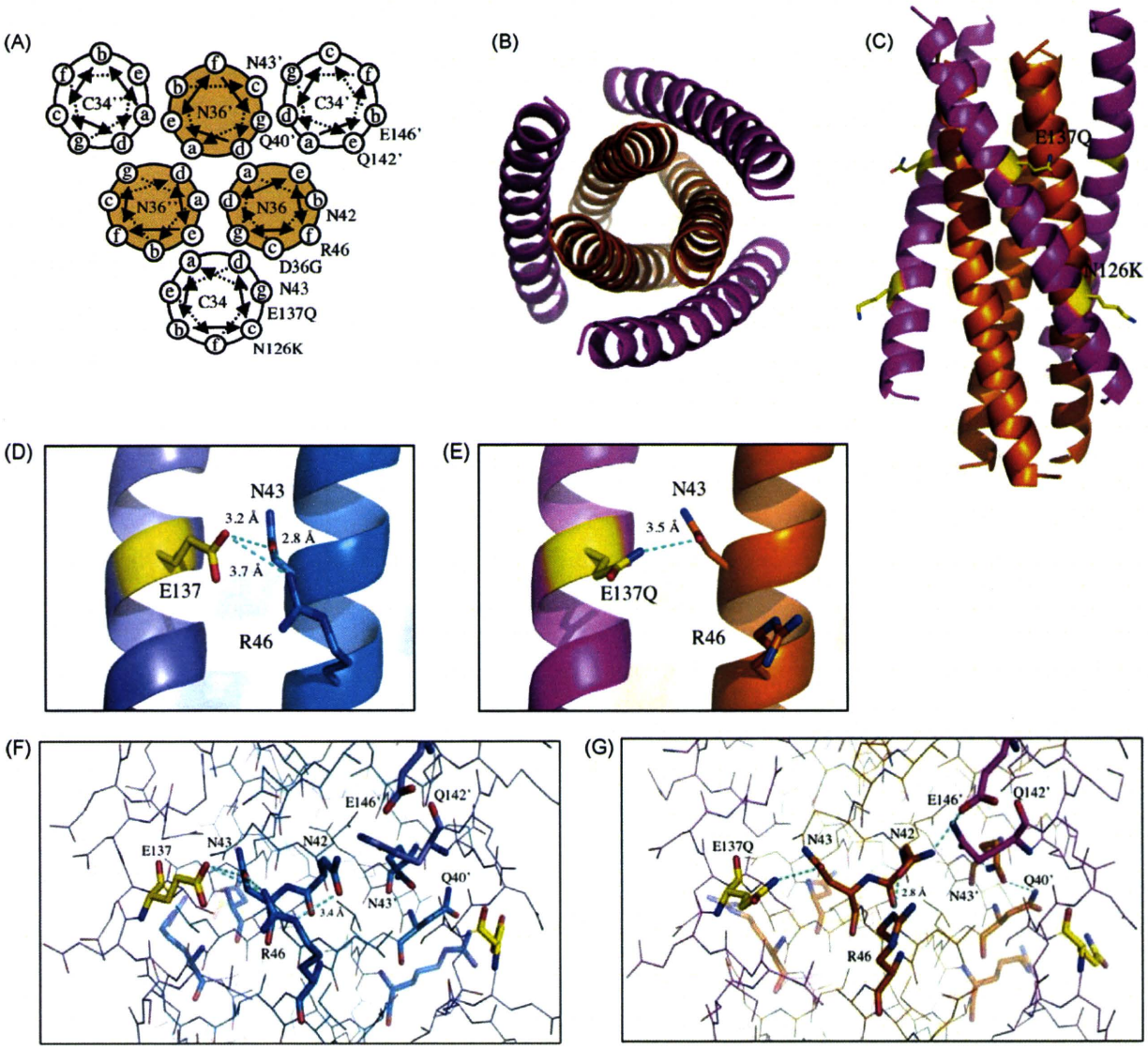

Fig. 4. Helical wheel representation of N36 and C34, and structure of N36-resistant HIV-1 gp41. The 6-helix bundle is represented as helical wheel projections (Chan et al., 1997) and the view is from the top of the complex. N36 and C34, N36′ and C34′, and N36″ and C34″ indicate each pair of a N36- and a C34-helix. The position of amino acid mutations in N36-resistant HIV-1 and the amino acids related to formation of hydrogen bonds is shown (A and B). (C) The entire structure of the 6-helix bundle with N126K and E137Q mutations. The views, focused on binding between an N36 and a C34 (D and F) and an N36 and a $C34_{KQ}$ (E and G), are shown. A hydrogen bond is depicted by the blue dashed line. (D) A hydroxyl group of the E137 side chain formed two hydrogen bonds with the amide oxygen of N43 and the amine of R46. A hydrogen bond also formed between the amide oxygen of N43 and the amine of R46. (E) The amide hydrogen of the E137Q side chain sustains a hydrogen bond with the amide oxygen of N43. The hydrogen bond formed between the amide hydrogen of E137Q and the amine of R46 was lost. The hydrogen bond formed between the amide oxygen of N43 and the amine of R46 in N36 was also lost. The views, focused on the hydrogen bond in the entire 6-helix bundle, formed with N36 and C34 (F) and N36 and $C34_{KQ}$ (G) are shown. A hydrogen bond is depicted by a blue dashed line. An apostrophe, upper right of an amino acid, means the amino acids of a neighboring helix pair as indicated in (A).

Table 2
Antiviral activity of HIV-1 gp41-derived peptides against recombinant viruses.

Viruses	EC_{50} [a] (nM)			
	ddC	DS5000	C34	N36
HIV-1_{WT}	505 ± 15[b]	56 ± 8.2	2.8 ± 1.2	200 ± 13
HIV-1_{D36G}	640 ± 76[c] (1.3)	94 ± 22 (1.7)	2.8 ± 1.2 (1)	250 ± 46 (1.3)
HIV-1_{N126K}	515 ± 86 (1)	88 ± 19 (1.5)	11 ± 3.1 (4)	550 ± 105 (2.8)
HIV-1_{E137Q}	500 ± 90 (1)	84 ± 14 (1.5)	3.0 ± 1.0 (1.1)	636 ± 159 (3.2)
HIV-$1_{N126K/E137Q}$	642 ± 84 (1.3)	74 ± 6.0 (1.3)	12 ± 4.7 (4.4)	731 ± 121 (3.7)
HIV-$1_{D36G/N126K/E137Q}$	728 ± 29 (1.4)	40 ± 4.0 (0.7)	15 ± 1.0 (5.2)	796 ± 144 (4)
HIV-$1_{gp120\text{-}P183Q}$	414 ± 50 (0.8)	58 ± 7.5 (1)	2.7 ± 0.6 (1)	343 ± 76 (1.7)
HIV-$1_{gp120\text{-}P183Q/D36G/N126K/E137Q}$	634 ± 150 (1.2)	43 ± 5.7 (0.8)	15 ± 2.4 (5.2)	573 ± 64 (2.9)

[a] Anti-HIV activity was determined with the MAGI assay.
[b] The data shown are mean value and standard deviation (SD) obtained from the results of at least three independent experiments.
[c] Values in parentheses represent fold-resistance in EC_{50} for recombinant viruses compared to HIV-1_{WT}.

faster entry kinetics shows resistance to T-20 (Reeves et al., 2002; Heredia et al., 2007; Hermann et al., 2009). However, only CCR5 tropic HIV-1s were subjected to be examined the entry kinetics and T-20 susceptibility in these studies, while CXCR4 tropic HIV-1s have been less examined yet. Interestingly, cell surface expression level of CCR5 influenced T-20 susceptibility but those of CD4 did not (Heredia et al., 2007), suggesting that entry kinetics of HIV-1 only through CCR5 influences T-20 susceptibility. In contrast, our study and others also revealed that D36G, the faster virus with CXCR4 tropism, showed high susceptibility to T-20 (Ueno et al., 2009; Mink et al., 2005; Kinomoto et al., 2005). In the present study, the faster viruses with mutations, such as P183Qand D36G little provided N36 resistance (Table 2). Thus, it is likely that there are some unknown differences in fusion inhibitor susceptibility between CXCR4 and CCR5 tropic viruses. As one of possibilities, Kahle et al. (2009) reported interesting data that asymmetric deactivation is observed in the C-HR targeted 5-helix peptide. Activity of the C-HR-derived peptide, C37 is well-correlated with binding affinity to the N-HR (K_D value), while that of 5-helix targeted the C-HR is poorly-correlated. They proposed a novel mechanism of fusion inhibition that peptides targeting N-HR and C-HR have distinctively reversible and irreversible deactivation of gp41 function, respectively.

D36G is one of the characteristic substitutions or polymorphisms for HIV-$1_{NL4\text{-}3}$, since only HIV-$1_{NL4\text{-}3}$ has D36 and others originally contains G36 (Kuiken et al., 2009). Kinomoto et al. (2009) analyzed D36G effect in a structure modeling with SIV gp41 and revealed D36 could induce distortion or incorrect positioning of the N and C helices by misdirected salt bridge with K144. However, less difference between the N36 conformations of wild-type and D36G mutant was expected, since the D36G, the second amino acid from the N-terminal end of N36, is located in the flexible region of N36 sequence. Experiments with the N-HR-derived peptide including expanded N-terminal region of N36 will be needed to reveal structural feature of D36G in the N-HR. In addition to a role in the viral entry, D36G has another role in viral replication kinetics as nucleotides ($D_{GAU}36G_{GGU}$) in the stem II_C of Rev responsive element (Ueno et al., 2009; Nameki et al., 2005). Nameki et al. (2005) demonstrated that $A_{GCC}30V_{GUC}$ located outside of the N-HR but complementally with $D_{GAU}36$ in the stem II_C, also enhanced replication kinetics of HIV-$1_{NL4\text{-}3}$ (underlined nucleotides; complementally located in the stem II_C) through compensation of the RNA structure. As such, D36G has at least 2 advantages, fusion and RNA stability for viral replication. In the present study, we, therefore, focused mainly on mutations in the C-HR region. In the CD analysis, enhanced 6-helix bundle stability of $N36/C34_{KQ}$ was observed, while structural alteration of the 6-helix bundle was not apparent. We hypothesize that the mechanism of resistance to N36 has little association with the binding ability of C-HR. Although the resistance of HIV-1 to C-HR-derived peptides accounts for a correlation with the binding affinity of N-HR, an important factor in the resistance to N36 may exist before completion of 6-helix bundle formation. Steger et al. reported that the 5-helix fusion inhibitor, containing three N-HR and two C-HR segments, targeting the C-HR region in gp41 as well as N36, demonstrated poor correlation between inhibitory potency and interaction affinity with C-HR (Steger and Root, 2006). The IC_{50} values of 5-helix variants with some mutations in the sequence were inversely proportional to their association rate constants. It is consistent with observations by Kahle et al. (2009) mentioned above that mechanism of inhibition of peptides targeting the N- and C-HRs seems to be different, deactivation of gp41 function and dominant negative/decoy effect, respectively. The anti-HIV activity of N36, which has the same target as the 5-helix variants, might be also correlated with association rate constants to C-HR and finally irreversibly deactivate the gp41 function.

In conclusion, non-aggregating and trimeric coiled-coil N-HR-derived peptides such as $(CCIZN17)_3$ have been developed and exhibit more potent anti-HIV-1 activity (Bianchi et al., 2005; Eckert and Kim, 2001a), as well as exerting a strong synergistic effect with T-20 (Bianchi et al., 2005). Therefore, N-HR-derived peptides with appropriate modifications are promising because of possible co-administration with T-20 and modulation of the resistance profile. The mechanism of resistance to N36, described in this paper, provides a role for the N126K and E137Q mutations in 6-helix bundle stability, although N126 does not directly associate with the N36 surface. Further experiments are needed to clarify the role of the common N126K mutation in HIV-1 fusion.

Acknowledgments

This work was supported in part by a grant for the Promotion of AIDS Research from the Ministry of Health and Welfare and the Ministry of Education, Culture, Sports, Science, and Technology of Japan (E.K. and S.O.); and a grant for Research for Health Sciences Focusing on Drug Innovation from The Japan Health Sciences Foundation (E.K., S.O., N.F. and M.M.).

References

Aquaro, S., D'Arrigo, R., Svicher, V., Di Perri, G., Lo Caputo, S., Visco-Comandini, U., Santoro, M., Bertoli, A., Mazzotta, F., Bonora, S., Tozzi, V., Bellagamba, R., Zaccarelli, M., Narciso, P., Antinori, A., Perno, C.F., 2006. Specific mutations in HIV-1 gp41 are associated with immunological success in HIV-1-infected patients receiving enfuvirtide treatment. J. Antimicrob. Chemother..

Armand-Ugon, M., Gutierrez, A., Clotet, B., Este, J.A., 2003. HIV-1 resistance to the gp41-dependent fusion inhibitor C-34. Antiviral Res. 59 (2), 137–142.

Bai, X., Wilson, K.L., Seedorff, J.E., Ahrens, D., Green, J., Davison, D.K., Jin, L., Stanfield-Oakley, S.A., Mosier, S.M., Melby, T.E., Cammack, N., Wang, Z., Greenberg, M.L., Dwyer, J.J., 2008. Impact of the enfuvirtide resistance mutation N43D and the associated baseline polymorphism E137K on peptide sensitivity and six-helix bundle structure. Biochemistry.

Baldwin, C.E., Sanders, R.W., Deng, Y., Jurriaans, S., Lange, J.M., Lu, M., Berkhout, B., 2004. Emergence of a drug-dependent human immunodeficiency virus type 1 variant during therapy with the T20 fusion inhibitor. J. Virol. 78 (22), 12428–12437.

Bianchi, E., Finotto, M., Ingallinella, P., Hrin, R., Carella, A.V., Hou, X.S., Schleif, W.A., Miller, M.D., Geleziunas, R., Pessi, A., 2005. Covalent stabilization of coiled coils of the HIV gp41 N region yields extremely potent and broad inhibitors of viral infection. Proc. Natl. Acad. Sci. U.S.A. 102 (36), 12903–12908.

Bienvenu, B., Krivine, A., Rollot, F., Pietri, M.P., Lebault, V., Meritet, J.F., Guerin, C., Spiridon, G., Salmon, D., Guillevin, L., Lebon, P., Launay, O., 2006. A cohort study of enfuvirtide immunological and virological efficacy in clinical practice. J. Med. Virol. 78 (10), 1312–1317.

Brunger, A.T., Adams, P.D., Clore, G.M., DeLano, W.L., Gros, P., Grosse-Kunstleve, R.W., Jiang, J.S., Kuszewski, J., Nilges, M., Pannu, N.S., Read, R.J., Rice, L.M., Simonson, T., Warren, G.L., 1998. Crystallography & NMR system: a new software suite for macromolecular structure determination. Acta Crystallogr. D: Biol. Crystallogr. 54 (Pt 5), 905–921.

Cabrera, C., Marfil, S., Garcia, E., Martinez-Picado, J., Bonjoch, A., Bofill, M., Moreno, S., Ribera, E., Domingo, P., Clotet, B., Ruiz, L., 2006. Genetic evolution of gp41 reveals a highly exclusive relationship between codons 36, 38 and 43 in gp41 under long-term enfuvirtide-containing salvage regimen. AIDS 20 (16), 2075–2080.

Chan, D.C., Chutkowski, C.T., Kim, P.S., 1998. Evidence that a prominent cavity in the coiled coil of HIV type 1 gp41 is an attractive drug target. Proc. Natl. Acad. Sci. U.S.A. 95 (26), 15613–15617.

Chan, D.C., Fass, D., Berger, J.M., Kim, P.S., 1997. Core structure of gp41 from the HIV envelope glycoprotein. Cell 89 (2), 263–273.

Desmezieres, E., Gupta, N., Vassell, R., He, Y., Peden, K., Sirota, L., Yang, Z., Wingfield, P., Weiss, C.D., 2005. Human immunodeficiency virus (HIV) gp41 escape mutants: cross-resistance to peptide inhibitors of HIV fusion and altered receptor activation of gp120. J. Virol. 79 (8), 4774–4781.

Dubay, J.W., Roberts, S.J., Brody, B., Hunter, E., 1992. Mutations in the leucine zipper of the human immunodeficiency virus type 1 transmembrane glycoprotein affect fusion and infectivity. J. Virol. 66 (8), 4748–4756.

Dwyer, J.J., Wilson, K.L., Martin, K., Seedorff, J.E., Hasan, A., Medinas, R.J., Davison, D.K., Feese, M.D., Richter, H.T., Kim, H., Matthews, T.J., Delmedico, M.K., 2008. Design of an engineered N-terminal HIV-1 gp41 trimer with enhanced stability and potency. Protein Sci. 17 (4), 633–643.

Dwyer, J.J., Wilson, K.L., Davison, D.K., Freel, S.A., Seedorff, J.E., Wring, S.A., Tvermoes, N.A., Matthews, T.J., Greenberg, M.L., Delmedico, M.K., 2007. Design of helical, oligomeric HIV-1 fusion inhibitor peptides with potent activity against enfuvirtide-resistant virus. Proc. Natl. Acad. Sci. U.S.A. 104 (31), 12772–12777.

Eckert, D.M., Kim, P.S., 2001a. Design of potent inhibitors of HIV-1 entry from the gp41 N-peptide region. Proc. Natl. Acad. Sci. U.S.A. 98 (20), 11187–11192.

Eckert, D.M., Kim, P.S., 2001b. Mechanisms of viral membrane fusion and its inhibition. Annu. Rev. Biochem. 70, 777–810.

Eggink, D., Baldwin, C.E., Deng, Y., Langedijk, J.P., Lu, M., Sanders, R.W., Berkhout, B., 2008. Selection of T1249-resistant human immunodeficiency virus type 1 variants. J. Virol. 82 (13), 6678–6688.

Eron, J.J., Gulick, R.M., Bartlett, J.A., Merigan, T., Arduino, R., Kilby, J.M., Yangco, B., Diers, A., Drobnes, C., DeMasi, R., Greenberg, M., Melby, T., Raskino, C., Rusnak, P., Zhang, Y., Spence, R., Miralles, G.D., 2004. Short-term safety and antiretroviral activity of T-1249, a second-generation fusion inhibitor of HIV. J. Infect. Dis. 189 (6), 1075–1083.

Fikkert, V., Cherepanov, P., Van Laethem, K., Hantson, A., Van Remoortel, B., Pannecouque, C., De Clercq, E., Debyser, Z., Vandamme, A.M., Witvrouw, M., 2002. Env chimeric virus technology for evaluating human immunodeficiency virus susceptibility to entry inhibitors. Antimicrob. Agents Chemother. 46 (12), 3954–3962.

Heredia, A., Gilliam, B., DeVico, A., Le, N., Bamba, D., Flinko, R., Lewis, G., Gallo, R.C., Redfield, R.R., 2007. CCR5 density levels on primary CD4 T cells impact the replication and Enfuvirtide susceptibility of R5 HIV-1. AIDS 21 (10), 1317–1322.

Hermann, F.G., Egerer, L., Brauer, F., Gerum, C., Schwalbe, H., Dietrich, U., von Laer, D., 2009. Mutations in gp120 contribute to the resistance of human immunodeficiency virus type 1 to membrane-anchored C-peptide maC46. J. Virol. 83 (10), 4844–4853.

Izumi, K., Kodama, E., Shimura, K., Sakagami, Y., Watanabe, K., Ito, S., Watabe, T., Terakawa, Y., Nishikawa, H., Sarafianos, S.G., Kitaura, K., Oishi, S., Fujii, N., Matsuoka, M., 2009. Design of peptide-based inhibitors for human immunodeficiency virus type 1 strains resistant to T-20. J. Biol. Chem. 284 (8), 4914–49120.

Kahle, K.M., Steger, H.K., Root, M.J., 2009. Asymmetric deactivation of HIV-1 gp41 following fusion inhibitor binding. PLoS Pathog. 5 (11), e1000674.

Kilby, J.M., Hopkins, S., Venetta, T.M., DiMassimo, B., Cloud, G.A., Lee, J.Y., Alldredge, L., Hunter, E., Lambert, D., Bolognesi, D., Matthews, T., Johnson, M.R., Nowak, M.A., Shaw, G.M., Saag, M.S., 1998. Potent suppression of HIV-1 replication in humans by T-20, a peptide inhibitor of gp41-mediated virus entry. Nat. Med. 4 (11), 1302–1307.

Kinomoto, M., Yokoyama, M., Sato, H., Kojima, A., Kurata, T., Ikuta, K., Sata, T., Tokunaga, K., 2005. Amino acid 36 in the human immunodeficiency virus type 1 gp41 ectodomain controls fusogenic activity: implications for the molecular mechanism of viral escape from a fusion inhibitor. J. Virol. 79 (10), 5996–6004.

Kuiken, C., Leitner, T., Foley, B., Hahn, B., Marx, McCutchan, F., Wolinsky, S., Korber, B., 2009. HIV sequence compendium, 2009. Theoretical Biology and Biophysics Group. Los Alamos National Laboratory, Los Alamos, NM.

Labrosse, B., Morand-Joubert, L., Goubard, A., Rochas, S., Labernardiere, J.L., Pacanowski, J., Meynard, J.L., Hance, A.J., Clavel, F., Mammano, F., 2006. Role of the envelope genetic context in the development of enfuvirtide resistance in human immunodeficiency virus type 1-infected patients. J. Virol. 80 (17), 8807–8819.

Lalezari, J.P., Henry, K., O'Hearn, M., Montaner, J.S., Piliero, P.J., Trottier, B., Walmsley, S., Cohen, C., Kuritzkes, D.R., Eron Jr., J.J., Chung, J., DeMasi, R., Donatacci, L., Drobnes, C., Delehanty, J., Salgo, M., 2003. Enfuvirtide, an HIV-1 fusion inhibitor, for drug-resistant HIV infection in North and South America. N. Engl. J. Med. 348 (22), 2175–2185.

Lazzarin, A., Clotet, B., Cooper, D., Reynes, J., Arasteh, K., Nelson, M., Katlama, C., Stellbrink, H.J., Delfraissy, J.F., Lange, J., Huson, L., DeMasi, R., Wat, C., Delehanty, J., Drobnes, C., Salgo, M., 2003. Efficacy of enfuvirtide in patients infected with drug-resistant HIV-1 in Europe and Australia. N. Engl. J. Med. 348 (22), 2186–2195.

Lohrengel, S., Hermann, F., Hagmann, I., Oberwinkler, H., Scrivano, L., Hoffmann, C., von Laer, D., Dittmar, M.T., 2005. Determinants of human immunodeficiency virus type 1 resistance to membrane-anchored gp41-derived peptides. J. Virol. 79 (16), 10237–10246.

Lu, M., Blacklow, S.C., Kim, P.S., 1995. A trimeric structural domain of the HIV-1 transmembrane glycoprotein. Nat. Struct. Biol. 2 (12), 1075–1082.

Lu, M., Ji, H., Shen, S., 1999. Subdomain folding and biological activity of the core structure from human immunodeficiency virus type 1 gp41: implications for viral membrane fusion. J. Virol. 73 (5), 4433–4438.

Lu, M., Kim, P.S., 1997. A trimeric structural subdomain of the HIV-1 transmembrane glycoprotein. J. Biomol. Struct. Dyn. 15 (3), 465–471.

McRee, D.E., 1999. XtalView/Xfit—a versatile program for manipulating atomic coordinates and electron density. J. Struct. Biol. 125 (2–3), 156–165.

Menzo, S., Castagna, A., Monachetti, A., Hasson, H., Danise, A., Carini, E., Bagnarelli, P., Lazzarin, A., Clementi, M., 2004. Genotype and phenotype patterns of human immunodeficiency virus type 1 resistance to enfuvirtide during long-term treatment. Antimicrob. Agents Chemother. 48 (9), 3253–3259.

Mink, M., Mosier, S.M., Janumpalli, S., Davison, D., Jin, L., Melby, T., Sista, P., Erickson, J., Lambert, D., Stanfield-Oakley, S.A., Salgo, M., Cammack, N., Matthews, T., Greenberg, M.L., 2005. Impact of human immunodeficiency virus type 1 gp41 amino acid substitutions selected during enfuvirtide treatment on gp41 binding and antiviral potency of enfuvirtide in vitro. J. Virol. 79 (19), 12447–12454.

Nameki, D., Kodama, E., Ikeuchi, M., Mabuchi, N., Otaka, A., Tamamura, H., Ohno, M., Fujii, N., Matsuoka, M., 2005. Mutations conferring resistance to human immunodeficiency virus type 1 fusion inhibitors are restricted by gp41 and Rev-responsive element functions. J. Virol. 79 (2), 764–770.

Nishikawa, H., Nakamura, S., Kodama, E., Ito, S., Kajiwara, K., Izumi, K., Sakagami, Y., Oishi, S., Ohkubo, T., Kobayashi, Y., Otaka, A., Fujii, N., Matsuoka, M., 2009. Electrostatically constrained alpha-helical peptide inhibits replication of HIV-1 resistant to enfuvirtide. Int. J. Biochem. Cell Biol. 41 (4), 891–899.

Otaka, A., Nakamura, M., Nameki, D., Kodama, E., Uchiyama, S., Nakamura, S., Nakano, H., Tamamura, H., Kobayashi, Y., Matsuoka, M., Fujii, N., 2002. Remodeling of gp41-C34 peptide leads to highly effective inhibitors of the fusion of HIV-1 with target cells. Angew. Chem. Int. Ed. Engl. 41 (16), 2937–2940.

Perez-Alvarez, L., Carmona, R., Ocampo, A., Asorey, A., Miralles, C., Perez de Castro, S., Pinilla, M., Contreras, G., Taboada, J.A., Najera, R., 2006. Long-term monitoring of genotypic and phenotypic resistance to T20 in treated patients infected with HIV-1. J. Med. Virol. 78 (2), 141–147.

Ray, N., Harrison, J.E., Blackburn, L.A., Martin, J.N., Deeks, S.G., Doms, R.W., 2007. Clinical resistance to enfuvirtide does not affect susceptibility of human immunodeficiency virus type 1 to other classes of entry inhibitors. J. Virol. 81 (7), 3240–3250.

Rimsky, L.T., Shugars, D.C., Matthews, T.J., 1998. Determinants of human immunodeficiency virus type 1 resistance to gp41-derived inhibitory peptides. J. Virol. 72 (2), 986–993.

Reeves, J.D., Gallo, S.A., Ahmad, N., Miamidian, J.L., Harvey, P.E., Sharron, M., Pohlmann, S., Sfakianos, J.N., Derdeyn, C.A., Blumenthal, R., Hunter, E., Doms, R.W., 2002. Sensitivity of HIV-1 to entry inhibitors correlates with envelope/coreceptor affinity, receptor density, and fusion kinetics. Proc. Natl. Acad. Sci. U.S.A. 99 (25), 16249–16254.

Steger, H.K., Root, M.J., 2006. Kinetic dependence to HIV-1 entry inhibition. J. Biol. Chem. 281 (35), 25813–25821.

Tolstrup, M., Selzer-Plon, J., Laursen, A.L., Bertelsen, L., Gerstoft, J., Duch, M., Pedersen, F.S., Ostergaard, L., 2007. Full fusion competence rescue of the enfuvirtide resistant HIV-1 gp41 genotype (43D) by a prevalent polymorphism (137K). AIDS 21 (4), 519–521.

Ueno, M., Kodama, E.N., Shimura, K., Sakurai, Y., Kajiwara, K., Sakagami, Y., Oishi, S., Fujii, N., Matsuoka, M., 2009. Synonymous mutations in stem-loop III of Rev responsive elements enhance HIV-1 replication impaired by primary mutations for resistance to enfuvirtide. Antiviral Res. 82 (1), 67–72.

Vagin, A., Teplyakov, A., 1997. MOLREP: an Automated Program for Molecular Replacement. J. Appl. Crystallogr. 30 (Pt 6), 1022–1025.

Wei, X., Decker, J.M., Liu, H., Zhang, Z., Arani, R.B., Kilby, J.M., Saag, M.S., Wu, X., Shaw, G.M., Kappes, J.C., 2002. Emergence of resistant human immunodeficiency virus type 1 in patients receiving fusion inhibitor (T-20) monotherapy. Antimicrob. Agents Chemother. 46 (6), 1896–1905.

Wild, C., Dubay, J.W., Greenwell, T., Baird Jr., T., Oas, T.G., McDanal, C., Hunter, E., Matthews, T., 1994. Propensity for a leucine zipper-like domain of human immunodeficiency virus type 1 gp41 to form oligomers correlates with a role

in virus-induced fusion rather than assembly of the glycoprotein complex. Proc. Natl. Acad. Sci. U.S.A. 91 (26), 12676–12680.
Wild, C., Greenwell, T., Matthews, T., 1993. A synthetic peptide from HIV-1 gp41 is a potent inhibitor of virus-mediated cell–cell fusion. AIDS Res. Hum. Retroviruses 9 (11), 1051–1053.
Wild, C., Oas, T., McDanal, C., Bolognesi, D., Matthews, T., 1992. A synthetic peptide inhibitor of human immunodeficiency virus replication: correlation between solution structure and viral inhibition. Proc. Natl. Acad. Sci. U.S.A. 89 (21), 10537–10541.

The International Journal of Biochemistry & Cell Biology 42 (2010) 1482–1488

Contents lists available at ScienceDirect

The International Journal of Biochemistry & Cell Biology

journal homepage: www.elsevier.com/locate/biocel

Rev-derived peptides inhibit HIV-1 replication by antagonism of Rev and a co-receptor, CXCR4

Kazuki Shimane[a,b], Eiichi N. Kodama[a,c,*], Ikuhiko Nakase[d], Shiroh Futaki[d], Yasuteru Sakurai[a,b], Yasuko Sakagami[a], Xiaoguang Li[c], Toshio Hattori[c], Stefan G. Sarafianos[e], Masao Matsuoka[a]

[a] *Laboratory of Virus Control, Institute for Virus Research, Kyoto University, Kyoto 606-8507, Japan*
[b] *Graduate School of Biostudies, Kyoto University, Kyoto 606-8501, Japan*
[c] *Tohoku University Graduate School of Medicine, Department of Internal Medicine/Division of Emerging Infectious Diseases, Sendai 980-8575, Japan*
[d] *Institute for Chemical Research, Kyoto University, Kyoto 611-0011, Japan*
[e] *Department of Molecular Microbiology and Immunology, University of Missouri School of Medicine, 471d C. Bond Life Sciences Center, Columbia, MO, United States*

ARTICLE INFO

Article history:
Received 1 February 2010
Received in revised form 23 April 2010
Accepted 11 May 2010
Available online 16 May 2010

Keywords:
HIV-1
Rev
CXCR4
Inhibitor
Alpha-helix

ABSTRACT

Rev, a viral regulatory protein of HIV-1, binds through its arginine-rich domain to the Rev-responsive element (RRE), a secondary structure in transcribed HIV-1 RNA. Binding of Rev to RRE mediates export of singly spliced or unspliced mRNAs from the nucleus to the cytoplasm. It has been previously shown that a certain arginine-rich peptide exhibits not only RRE-binding ability but also cell permeability and antagonism of CXCR4, one of the major coreceptors of HIV-1. Here we designed and synthesized arginine-rich peptides derived from the RNA-binding domain of Rev (Rev_{34-50}) and evaluated their anti-HIV-1 activities. Rev_{34-50}-A_4C, comprising Rev_{34-50} with AAAAC at the C-terminus to increase the α-helicity, inhibited HIV-1 entry by CXCR4 antagonism and virus production in persistently HIV-1-infected PM1-CCR5 cells. Interestingly, similar motif of human lymphotropic virus type I Rex (Rex_{1-21}) also exerted moderate anti-HIV-1 activity. These results indicate that arginine-rich peptide, Rev_{34-50}-A_4C exerts dual antagonism against CXCR4 and Rev.

1. Introduction

HIV-1 attaches to its target cells through a major receptor, CD4, and then interacts with coreceptors such as chemokine receptors to enter the cells (Este and Telenti, 2007). The T-cell-line-tropic (X4) and macrophage-tropic (R5) HIV-1 strains mainly use CXCR4 and CCR5 as coreceptors, respectively. HIV-1 completes its infection by integration of reverse-transcribed double-stranded cDNA into the host genome. Expression of HIV-1 genes is enhanced by the viral transactivator protein Tat, while regulation of the expressed genes through RNA splicing is tightly controlled by the viral regulatory protein Rev. Some expressed RNAs are protected against RNA splicing by binding of Rev to a Rev-responsive element (RRE), comprising an RNA secondary structure co-encoded with gp41, resulting in singly spliced (e.g., for *env* mRNA) or unspliced (e.g., for *gag-pol* mRNA or viral progeny genomes) RNAs, which are exported to the cytoplasm by Rev and used for viral protein synthesis and/or progeny genomes (Felber et al., 1989; Malim et al., 1989b).

Rev contains several functional signals, such as a nuclear localization signal (NLS; aa 35–50), which also serves as an RNA-binding domain (Malim and Cullen, 1991; Olsen et al., 1990), and a nuclear export signal (NES; aa 75–84) as shown in Fig. 1 (Fischer et al., 1995; Szilvay et al., 1995). The RNA structure of the RRE in these singly and unspliced RNAs plays an important role in the interaction with Rev (Charpentier et al., 1997; Dayton et al., 1989). Rev mainly binds to stem-loop IIB of the RRE and oligomerization of Rev on the RRE is required for sufficient RNA export (Daugherty et al., 2008; Kjems et al., 1992; Mann et al., 1994; Zapp et al., 1991). Another human retrovirus, human T-cell leukemia virus type I (HTLV-I), also has a regulatory protein, Rex, which is the counterpart of HIV-1 Rev. Rex interacts with not only a Rex-responsive element (RxRE) but also with the HIV-1 RRE via its RNA-binding domain (aa 1–16), which also acts as an NLS (Bogerd et al., 1991; Hammes and Greene, 1993; Siomi et al., 1988). Functionally, Rex is also involved in the nuclear export of RNAs containing an RxRE or RRE (Rimsky et al., 1988). However, Rex and Rev interact with the RRE in different manners, since Rev mainly binds to stem-loop IIB while Rex mainly binds to the stem-loop III/IV/V region (Ahmed et al., 1990; Bogerd et al., 1991; Charpentier et al., 1997; Kjems et al., 1992).

* Corresponding author at: Building 1 Room 515, Tohoku University Graduate School of Medicine, Department of Internal Medicine/Division of Emerging Infectious Diseases, 2-1 Seiryo-cho, Aoba-ku, Sendai 980-8575, Japan.
Tel.: +81 22 717 7199; fax: +81 22 717 8221.
E-mail address: kodama515@m.tains.tohoku.ac.jp (E.N. Kodama).

1357-2725/$ – see front matter © 2010 Elsevier Ltd. All rights reserved.
doi:10.1016/j.biocel.2010.05.005

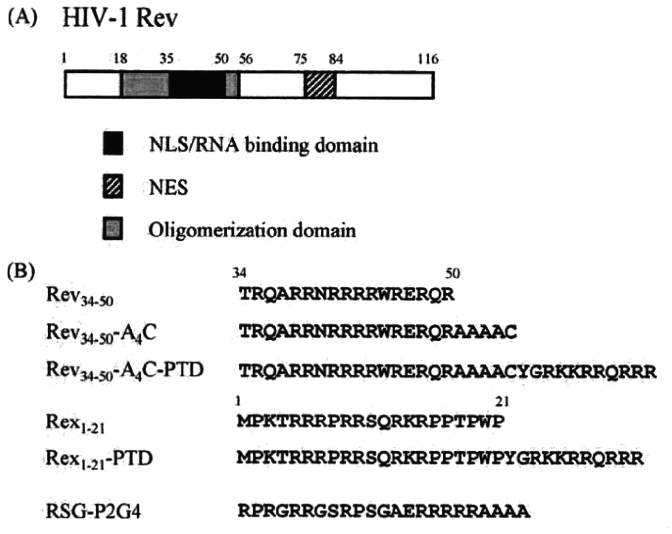

Fig. 1. Domain structure of HIV-1 Rev and sequences of Rev- and Rex-derived peptides. (A) Diagrammatic representation of HIV-1 Rev. The functional domains and regions of HIV-1 Rev are depicted. (B) Sequences of Rev-derived, Rex-derived and RSG-P2G4 peptides. The Rev- and Rex-derived peptides were synthesized based on the HIV-1_{NL4-3} (GenBank Accession No. AF324493) and HTLV-I MT-2 (GenBank Accession No. L03561) sequences, respectively. The protein transduction domain (PTD; YGRKKRRQRRR), an amino acid sequence derived from HIV-1_{NL4-3} Tat protein (aa 47–57), was added to the C-terminus of the peptides.

At least three properties seem to be required to antagonize Rev function: cell permeability, nuclear localization and specific binding to HIV-1 RRE or Rev. In this regard, Rev M10, a Rev mutant lacking the nuclear export activity, efficiently suppresses HIV-1 replication through a dominant-negative effect on Rev function (Malim et al., 1989a). However, it has several obstacles to overcome, such as immunogenicity, chemical synthesis and administration, for clinical application. In contrast, small peptides may be ideal for overcoming such obstacles. Harada et al. (1996, 1997) designed and examined artificial arginine-rich peptides as Rev antagonists in biochemical binding assays. The crystal structure of Rev/RRE has been reported (Jain and Belasco, 2001). Based on this structure (Jain and Belasco, 2001; Jiang et al., 1999), we designed peptides of 17 and 21 amino acids derived from the RRE-binding domains of Rev and Rex proteins, designated Rev_{34-50} and Rex_{1-21}, respectively, and examined their anti-HIV-1 activities. These peptides contain an arginine-rich domain, which not only binds to the RRE but also imparts cell permeability and nuclear localization (Futaki et al., 2001). Notably, it has been reported that arginine-rich peptides, e.g., ALX40-4C (N-α-acetyl-nona-D arginine), show anti-HIV-1 activity via antagonistic effects against CXCR4 (Doranz et al., 1997). We hypothesized that the arginine-rich RNA-binding domains of Rev and Rex inhibit both the entry of HIV-1 through CXCR4 and the production of progenitor HIV-1 by interrupting the function of Rev in the early and late phases of the replication cycle.

In this study, we tested this hypothesis by synthesizing Rev- and Rex-derived peptides based on their RNA-binding domains, as well as RSG-P2G4, an arginine-rich peptide that interacts with the RRE (Harada et al., 1997), and by evaluating their antiviral activities as bifunctional inhibitors that target Rev and CXCR4.

2. Materials and methods

2.1. Reagents

AZT was purchased from Sigma (St. Louis, MO). Amprenavir (APV) was kindly provided by Dr. H. Mitsuya (Kumamoto University, Kumamoto, Japan). AMD3100 was a kind gift from Dr. S. Shigeta (Fukushima Medical University, Fukushima, Japan). TAK-779 was obtained from the AIDS Research and Reference Program, Division of AIDS, National Institute of Allergy and Infectious Disease (Bethesda, MD). All peptides used in this study were chemically synthesized by Fmoc-solid-phase peptide synthesis on a Rink amide resin as reported previously (Futaki et al., 1997). A phycoerythrin (PE)-conjugated mouse anti-human CXCR4 MAb (12G5) was purchased from BD Bioscience Clontech (San Jose, CA).

2.2. Cells and viruses

Two laboratory strains, HIV-1_{IIIB} and HIV-1_{Ba-L}, that mainly interact with CXCR4 and CCR5 as coreceptors, respectively, were used in this study.

MT-2 cells were grown in RPMI 1640 medium (Sigma, St. Louis, MO). PM1-CCR5 cells, which are CCR5-transduced PM1 cells, and PM1-CCR5/IIIB and PM1-CCR5/Ba-L cells, which are PM1-CCR5 cells persistently infected with HIV-1_{IIIB} or HIV-1_{Ba-L}, respectively, were maintained in RPMI 1640 medium supplemented with G418 disulfide (0.5 mg/ml; Nacalai Tesque, Kyoto, Japan). HeLa CD4/CCR5/LTR-β-galactosidase (MAGI/CCR5) cells (Vodicka et al., 1997) were kindly provided by Dr. J. Overbaugh through the AIDS Research and Reference Program. MAGI/CCR5, 293T and NP-2 cells were maintained in Dulbecco's modified Eagle's medium (Sigma). All media were supplemented with 10% fetal calf serum (FCS), 2 mM L-glutamine, 100 U/ml penicillin and 50 μg/ml streptomycin.

2.3. Determination of anti-HIV-1 activity

The anti-HIV-1 activities of the peptides in the early phase of the replication cycle were determined by the MAGI assay as described previously (Nameki et al., 2005). The inhibitory effects of the peptides in the late phase were evaluated using PM1-CCR5 cells persistently infected with HIV-1. Briefly, PM1-CCR5/IIIB or PM1-CCR5/Ba-L cells were washed three times and resuspended at 4×10^4 cells/ml with the peptides in the RPMI 1640-based medium. After 48 h, the amounts of viral p24 antigen present in the culture supernatants were measured using a RETRO-TEK HIV-1 p24 Antigen ELISA Kit (ZeptoMetrix Corporation, Buffalo, NY). The cytotoxicities of the peptides were evaluated by a 3-(4,5-dimethylthiazol-2-yl)-2,5-diphenyltetrazolium bromide (MTT) colorimetric assay as described previously (Kodama et al., 2001).

2.4. Flow cytometric analysis of the antagonistic effects on CXCR4

MT-2 cells were resuspended in phosphate-buffered saline (PBS) containing 1% FCS and preincubated with peptides at 4 °C for 30 min. PE-conjugated anti-CXCR4 MAb (12G5) was then added and incubated at 4 °C for a further 30 min. The cells were washed three times, fixed with 1% formaldehyde and analyzed using an EPICS XL flow cytometer (Beckman Coulter, Miami Lakes, FL).

2.5. Evaluation of the anti-HIV-1 effects of intracellular expression of Rev peptides

We constructed pCI-Rev-IG vectors encoding various Rev mutants, an internal ribosomal entry site (IRES) and neomycin phosphotransferase ($G418^r$) under the control of a cytomegalovirus (CMV) promoter as shown in Fig. 4. The pCI-Rev-IG plasmids were transfected into MT-2 cells using the TransIT transfection reagent (Mirus Bio, Madison, WI). After 16 h, the transduced MT-2 cells were subjected to G418 selection, and further cultured in the presence of G418 (0.5 mg/ml).

Rev-transduced MT-2 cells were resuspended in 96-well plates (3×10^3 cells/well) and incubated with HIV-1_{IIIB}. After 5 days, the

cytopathic effects were determined by the MTT assay as described previously (Kodama et al., 2001).

2.6. Subcellular localizations of Rev and Rex peptides

To evaluate the subcellular localizations of Rev and Rex peptides, we constructed $pRev_{peptide}$-EGFP and $pRex_{peptide}$-EGFP vectors expressing C-terminally EGFP-fused peptides using pEGFP N1 (Clontech Laboratories Inc., Palo Alto, CA). The plasmids were transfected into 293T and NP-2 cells using the TransIT transfection reagent. After 48 h, the cells were fixed with 1% formaldehyde and examined with a BioZERO fluorescence microscope (BZ-8000; Keyence, Osaka, Japan).

3. Results

3.1. Arginine-rich peptides inhibit HIV-1_{IIIB} infection

The amino acid sequences of the peptides are shown in Fig. 1. The peptides were examined for their anti-HIV-1 activities by the MAGI assay (Table 1), which only detects anti-HIV-1 activity in the early phase of the replication cycle up to the point of Tat interaction with the long terminal repeat (LTR) within 48 h post viral inoculation (Uchida et al., 1997). The reverse transcriptase inhibitor zidovudine (AZT) inhibited both HIV-1_{IIIB} and HIV-1_{Ba-L}, which use CXCR4 and CCR5 as coreceptors, respectively, while AMD3100 and TAK-779, which are specific antagonists of CXCR4 or CCR5 (Baba et al., 1999; Donzella et al., 1998), only inhibited HIV-1_{IIIB} and HIV-1_{Ba-L}, respectively. All peptides showed anti-HIV-1 activity against HIV-1_{IIIB}, but not HIV-1_{Ba-L}. Addition of the 5 amino acids AAAAC (A_4C), which stabilizes the α-helical structure (Lin et al., 2004), to the C-terminus of Rev_{34-50} (Rev_{34-50}-A_4C) enhanced the activity against HIV-1_{IIIB} compared with the parental Rev_{34-50}. The anti-HIV-1 activity of Rev_{34-50}-A_4C was slightly enhanced by addition of the protein transduction domain of HIV-1 Tat (Tat-PTD) to the C-terminus (see Fig. 1B), which increases the intracellular delivery of the conjugated protein or peptide (Nagahara et al., 1998). Rex_{1-21} partially inhibited infection by HIV-1_{IIIB} at 10 μM (approximately 40%) and its anti-HIV-1 activity was increased by addition of Tat-PTD. Another arginine-rich peptide, RSG-P2G4 (Harada et al., 1997), also only inhibited HIV-1_{IIIB} infection.

Table 1
Anti-HIV-1 activities of Rev- and Rex-derived peptides[a].

Compound	EC_{50}[b] (μM)	
	HIV-1_{IIIB}	HIV-1_{Ba-L}
Rev_{34-50}	1.7 ± 0.25	>10
Rev_{34-50}-A_4C	0.35 ± 0.07	>10
Rev_{34-50}-A_4C-PTD	0.37 ± 0.09	>10
Rex_{1-21}	>10	>10
Rex_{1-21}-PTD	2.5 ± 0.76	>10
RSG-P2G4	2.2 ± 0.51	>10
AZT	0.022 ± 0.005	0.055 ± 0.009
AMD3100	0.0038 ± 0.0011	>100
TAK-779	>100	0.0030 ± 0.0019

[a] Anti-HIV-1 activity was determined by the MAGI assay that detects early phase of HIV replication (Uchida et al., 1997). HIV-1_{IIIB} and HIV-1_{Ba-L} are one of representative strains for CXCR4 and CCR5 tropic HIV-1.
[b] EC_{50}, 50% effective concentration. Data represent the means ± SD of at least three independent experiments.

3.2. Antagonism against CXCR4

It has been demonstrated that arginine-rich peptides bind to CXCR4, resulting in inhibitory effects on the binding of the HIV-1 gp120 V3 loop to CXCR4 (entry inhibition) (Doranz et al., 1997; Murakami et al., 1999). Our synthesized peptides contained an arginine-rich motif in their sequences and blocked early-phase infection only by the CXCR4-tropic HIV-1_{IIIB} virus. Therefore, we investigated whether the anti-HIV-1 activities of these peptides in the early phase were produced by CXCR4 antagonism using flow cytometric analysis with an anti-CXCR4 monoclonal antibody (MAb; 12G5). All the peptides, including Rev_{34-50}-A_4C, Rev_{34-50}-

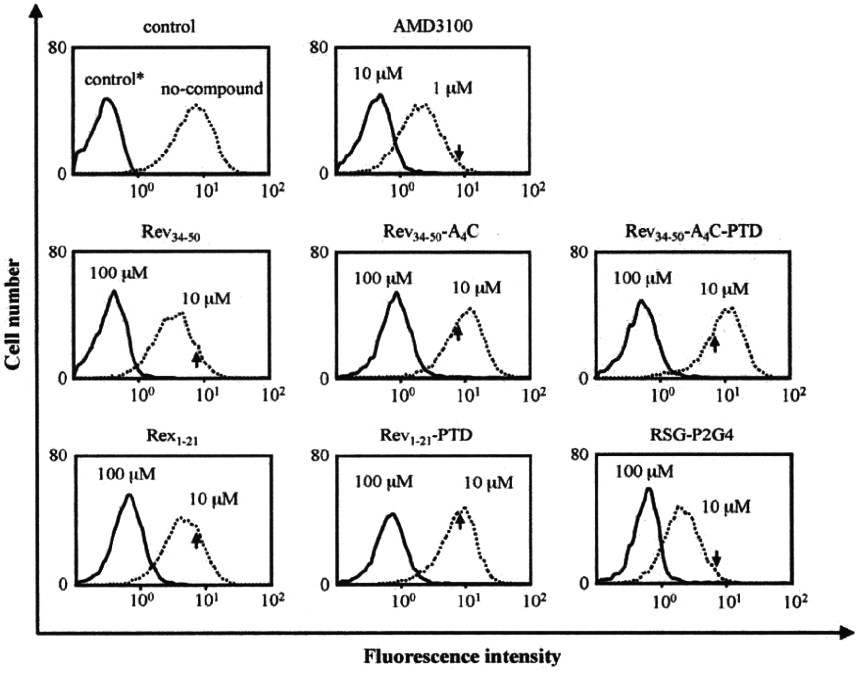

Fig. 2. Effects of the peptides on binding of a MAb against CXCR4 expressed on the MT-2 cell surface. MT-2 cells were resuspended in PBS containing 1% FCS and preincubated with the peptides at 4 °C for 30 min. PE-conjugated anti-CXCR4 MAb (12G5) was then added and incubated at 4 °C for a further 30 min. The cells were washed three times, fixed with 1% formaldehyde, and analyzed using a flow cytometer. A CXCR4 antagonist, AMD3100, was used a positive control. The results represent one of three independent experiments. (*) Fluorescence without PE-conjugated 12G5 is shown. Arrowhead indicates the mean fluorescence intensity of the no compound control.

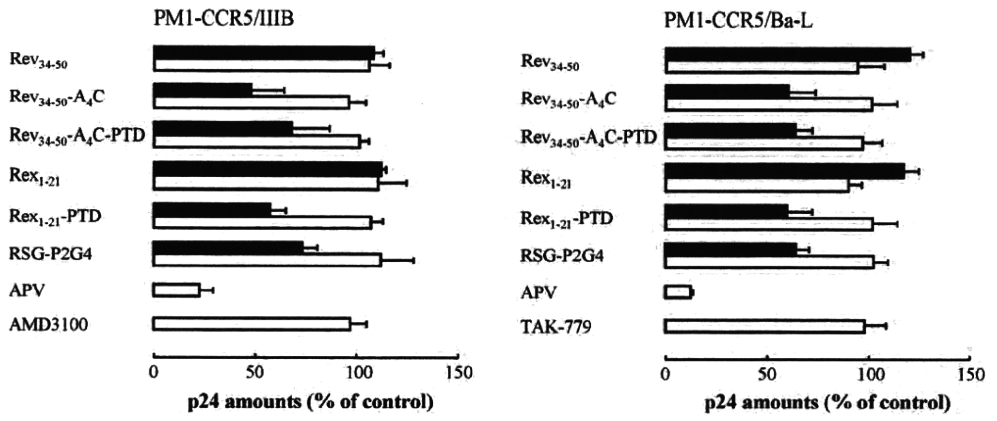

Fig. 3. Inhibitory effects of the peptides on p24 production from persistently HIV-1-infected PM1-CCR5 cells. PM1-CCR5 cells persistently infected with HIV-1_{IIIB} or HIV-1_{Ba-L} (PM1-CCR5/IIIB or PM1-CCR5/Ba-L cells, respectively) were washed and resuspended at 4×10^4 cells/ml with the peptides (black bars: 10 μM; white bars: 1 μM), APV as a positive control or AMD3100, TAK-779 or medium alone (control) as negative controls. After 48 h, the amounts of viral p24 in the culture supernatants were measured. The results are expressed as the percentages of p24 relative to that of the control. The data represent the means + SD of three independent experiments.

A_4C-PTD and Rex_{1-21}-PTD (data not shown), inhibited binding of 12G5 in a dose-dependent manner as observed for AMD3100 (Fig. 2). Although Rex_{1-21} showed only weak inhibitory activity against HIV-1_{IIIB} at 10 μM (data not shown), it blocked the binding of 12G5 sufficiently at 100 μM (Fig. 2). Relatively high concentrations of peptides were required to block binding of 12G5. It is likely that numerous functional and non-functional CXCR4 for HIV-1 infection may be expressed on the cell surface. In the CCR5 case, the antagonism observed in less than 20% of cell surface expressed CCR5 appeared to be sufficient for inhibition of HIV infection (Maeda et al., 2004), since only that to functional CCR5 as an HIV-1 receptor, including co-localization with CD4, appears to be required. However, for a flow cytometer analysis, monoclonal antibodies and small agents including peptides can recognize both functional and non-functional, therefore, high concentration seems to be needed. Actually, another peptide CXCR4 antagonist, T134 was also required high concentration to inhibit 12G5 binding in a flow cytometry (Arakaki et al., 1999). These results indicate that the arginine-rich peptides may inhibit infection by HIV-1_{IIIB} through antagonism for CXCR4.

3.3. Inhibitory effects against viral production

In addition of the CXCR4 antagonism, the inhibitory effects of the peptides in the late phase were independently evaluated using persistently HIV-1-infected PM1-CCR5 cells. AMD3100, TAK-779 and the protease inhibitor APV were used as controls. The specific CXCR4 or CCR5 antagonists AMD3100 and TAK-779, respectively, had no inhibitory effects on viral production, whereas APV (1 μM) effectively inhibited the production of viral p24 antigen from both PM1-CCR5/IIIB and PM1-CCR5/Ba-L cells (Fig. 3). Rev_{34-50}, which specifically binds to the RRE similar to intact Rev *in vitro* (Kjems et al., 1992), showed no inhibitory effects on the production of viral p24, whereas Rev_{34-50}-A_4C inhibited the production of p24 from both PM1-CCR5/IIIB and PM1-CCR5/Ba-L cells. Addition of Tat-PTD to Rev_{34-50}-A_4C, which provides cell permeability, hardly enhanced the inhibitory effect. On the other hand, although Rex_{1-21} had no effect on the production of viral p24, Rex_{1-21}-PTD inhibited the production of viral p24 from both PM1-CCR5/IIIB and PM1-CCR5/Ba-L cells. RSG-P2G4, which interacts with the RRE more tightly than Rev_{34-50} (Harada et al., 1997), also inhibited the production of p24 from both PM1-CCR5/IIIB and PM1-CCR5/Ba-L cells. However, the antiviral activities of Rev_{34-50}-A_4C, Rev_{34-50}-A_4C-PTD and Rex_{1-21}-PTD were comparable to that of RSG-P2G4. None of the peptides showed any cytotoxicity for 5 days, as evaluated by 3-(4,5-dimethylthiazol-2-yl)-2,5-diphenyltetrazolium bromide (MTT) assays (data not shown).

3.4. Infectivity of secreted HIV-1

To address whether HIV-1 secreted from the persistently infected PM-1 treated with peptides, maintains its infectivity, we examined the infectivity of HIV-1 particles in the supernatant. To avoid effect of CXCR4 antagonism by the peptides, we used HIV-1_{Ba-L} strain for the experiments. PM1-CCR5/Ba-L cells were washed 3 times and exposed to each peptide (10 μM) for 24 h. The supernatant, which contains newly produced and secreted HIV-1_{Ba-L}, was harvested and subjected to the titration with the MAGI cells and the p24 assay. $Rev_{3450A4C}$ attenuated the infectivity compared to the anticipated one by p24, while other peptides, Rev_{3450} and P2G4 showed moderately reduced infectivity (Table 2). However, both Rex-derived peptides showed little changes in actual and anticipated infectivity. These results indicate that the peptides, especially $Rev_{34-50}A_4C$, might sustain its binding to the RRE even in the virion and/or during RT reaction after the next round of the new infection, led to the reduced infectivity.

3.5. Anti-HIV-1 effects on intracellular expression of Rev peptides

The arginine-rich peptides inhibited the production of p24 in PM1-CCR5 cells persistently infected with HIV-1 (Fig. 3). Next, we evaluated the effects of intracellular expression of various Rev mutants in MT-2 cells against HIV-1 infection using MTT assays.

Table 2
Peptide effect on infectivity of HIV-1_{Ba-L}.

Compound	% of non-treated control		Infectivity/p24
	Infectivity	p24	
Rev_{34-50}	74 ± 11	119 ± 16	0.62
Rev_{34-50}-A_4C	24 ± 1	67 ± 8	0.36
Rex_{1-21}	121 ± 43	93 ± 24	1.3
Rex_{1-21}-PTD	74 ± 30	82 ± 15	0.97
RSG-P2G4	72 ± 32	92 ± 5	0.78

Infectivity and amount of p24 in the supernatant of PM1-CCR5/Ba-L cells exposed to peptides (10 μM) were determined by the MAGI assay and a commercially available p24 kit, respectively. Each value was normalized by that of simultaneously performed non-treated control as 100%. Data represent the means ± SD of three independent experiments.

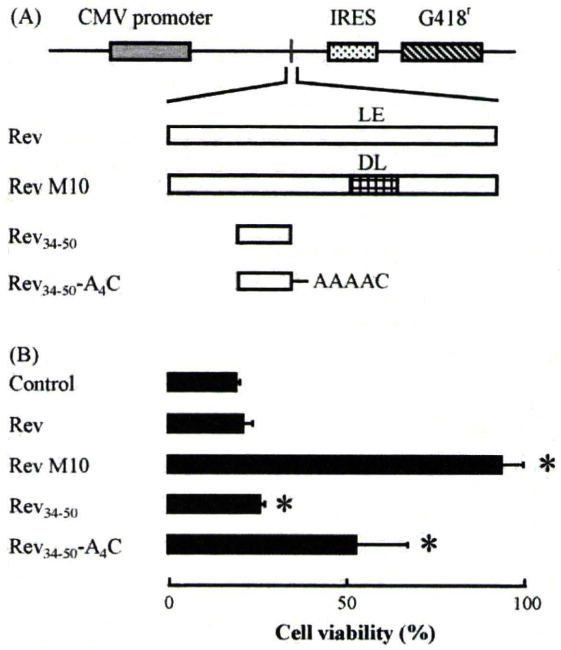

Fig. 4. Anti-HIV-1 activities of various Rev-transduced MT-2 cells. (A) Structures of the pCI-Rev-IG expression vectors encoding various Rev mutants. The fragments encoding Rev, Rev M10 ($D_{78}L_{79}$), Rev_{34-50} and Rev_{34-50}-A_4C were inserted into the upstream of IRES-$G418^r$ under the control of the CMV promoter. Amino acid substitutions at $L_{78}E_{79}$ (wild type Rev) to $D_{78}L_{79}$ (Rev dominant-negative mutant, Rev M10) diminish nuclear export of HIV mRNA (Malim and Cullen, 1991). (B) Effects of various Rev mutant transductions on HIV-1. MT-2 cells were transfected with various Rev mutant-encoding vectors and subjected to G418 selection. The Rev-transduced cells were infected with $HIV\text{-}1_{IIIB}$. On day 5 post-infection, the cell viabilities were determined by the MTT assay. The assays were performed in triplicate and the means + SD are shown. The results are representative of three independent experiments. $^*p < 0.05$, significant difference to the control by Student's *t*-test.

To obtain such MT-2 cells, the cells were transfected with various Rev expression vectors and then selected by G418. Although the expression of Rev hardly affected the cell death caused by HIV-1 infection, transduction of Rev M10, a dominant-negative mutant of Rev lacking NES activity, dramatically conferred resistance against HIV-1 infection (Fig. 4). Transduction of Rev_{34-50} moderately protected the cells. However, Rev_{34-50}-A_4C-transduced cells became more resistant to HIV-1 infection than Rev_{34-50}-transduced cells. These results for the transduced cells are consistent with those obtained for the persistently HIV-1-infected cells (Fig. 3). Therefore, the intracellular expression of Rev peptides conferred resistance against HIV-1 infection.

3.6. Subcellular localizations of Rev and Rex peptides

To elucidate the inhibitory mechanism of the arginine-rich peptides in the late phase of the replication cycle, we constructed $pRev_{peptide}$-EGFP and $pRex_{peptide}$-EGFP vectors expressing C-terminally EGFP-fused Rev and Rex peptides and examined the subcellular localizations of the EGFP-fused Rev and Rex peptides. In 293T cells, EGFP alone was equally distributed throughout the cells (Fig. 5, the 1st panel Control). In contrast, Rev and Rev M10 were mostly detected in nucleoli as previously reported (Dundr et al., 1995; Kalland et al., 1994; Stauber et al., 1995). Rev_{34-50}, Rev_{34-50}-A_4C and Rex_{1-21} were moderately detected in the cytoplasm, but dominantly accumulated in the nucleus. Similar results were observed in NP-2 cells (data not shown). These results indicate that Rev peptides exert antiviral activity in the same manner as Rev M10.

4. Discussion

4.1. Rev- and Rex-derived peptides act as dual antagonists toward CXCR4 and Rev

In the present study, we have demonstrated that arginine-rich peptides corresponding to the RRE-binding domains of HIV-1 Rev and HTLV-I Rex have dual inhibitory effects, namely CXCR4 antagonism and a dominant-negative effect for Rev function. Addition of A_4C, which stabilizes the α-helical structure (Lin et al., 2004), to Rev_{34-50} enhanced the inhibitory effects toward both CXCR4 antagonism and Rev function. It has been demonstrated that Rev_{34-50} forms an α-helical structure (Battiste et al., 1996; Tan et al., 1993) and binds to the RRE more efficiently when its α-helicity is increased (Tan et al., 1993). Short α-helical peptides (>20 amino acids) are known to have unstable helical structures and their helical structure is stabilized as their length increases (Marqusee et al., 1989). Hence, it is likely that the expected increase in α-helicity of Rev_{34-50} by the addition of A_4C resulted in enhanced CXCR4 antagonism and inhibition of p24 production at a post-transcriptional step for HIV-1 genes. The Rev peptides lacked NES activity, similar to the case of Rev M10, which is a trans-dominant repressor of Rev function (Malim et al., 1989a; Malim and Cullen, 1991). Therefore, the peptides may inhibit HIV-1 replication by competing with Rev for binding to the RRE, similar to the case of Rev M10. We observed that the Rev peptides, which contained a NLS, accumulated in the nucleoli. Expression of Rev M10 inhibited the cell death caused by HIV-1 significantly more efficiently than Rev_{34-50}-A_4C. This may be the result of Rev_{34-50}-A_4C being able to inhibit only the Rev-RRE binding step, whereas Rev M10 can inhibit multiple Rev functions

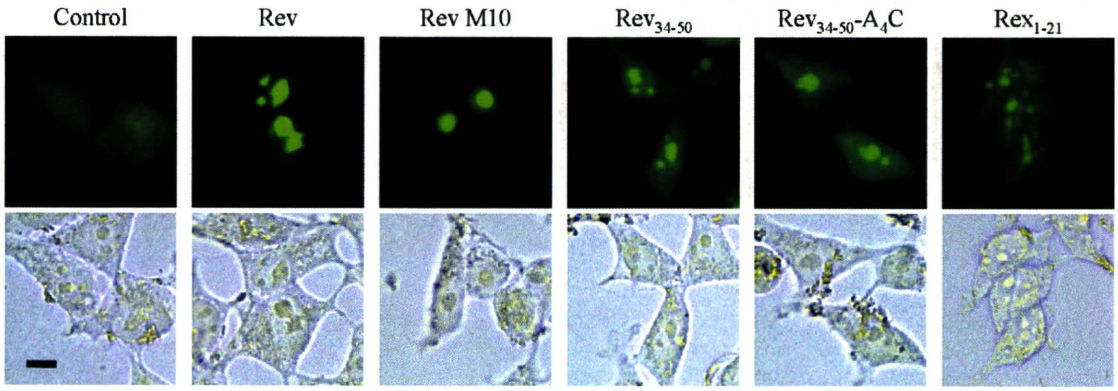

Fig. 5. Subcellular localizations of Rev and Rex peptides. 293T cells were transfected with $pRev_{peptide}$-EGFP and $pRex_{peptide}$-EGFP plasmids expressing Rev-, Rev M10-, Rev_{34-50}-, Rev_{34-50}-A_4C- and Rex_{1-21}-EGFP fusion proteins and EGFP alone as a control. After 48 h, the cells were fixed and examined using a fluorescence microscope (excitation: 488 nm). Fluorescent (upper panels) and corresponding phase-contrast (lower panels) images are shown. Scale bar: 10 μm.

by forming Rev-Rev M10 hetero-oligomers lacking NES activity (Stauber et al., 1995). However, despite the higher potency of Rev M10, its clinical applications are limited because it only differs from Rev by two amino acids. In this regard, the short peptide Rev_{34-50}-A_4C is more well suited for clinical applications. In fact, enfuvirtide (T-20), a similar 36-amino acid long peptide which inhibits HIV-1 fusion has been approved for the treatment of HIV infections and its clinical efficacy and utility has been demonstrated (Lalezari et al., 2003; Lazzarin et al., 2003).

Although addition of Tat-PTD may enhance the cell permeability of the peptides, its effects on cell permeability may be limited because the Rev and Rex peptides showed efficient cell permeability, as previously described (Futaki et al., 2001). It has been reported (Futaki et al., 2001) that peptides containing 6 and 8 arginine residues show efficient cell permeability. It is likely that addition of Tat-PTD to Rev_{34-50}-A_4C or Rex_{1-21}-A_4C hardly affected their cell permeability, as they already contained a large number of arginines. Notably, Tat-PTD does not interact with the RRE (Harada et al., 1996). On the other hand, Rex_{1-21} itself has sufficient cell permeability (Futaki et al., 2001), and addition of Tat-PTD to Rex_{1-21} enhanced its inhibitory activity likely through interactions with the CXCR4 coreceptor. Specifically, although Rex_{1-21} showed a weak antagonistic effect against CXCR4 by itself, addition of Tat-PTD to Rex_{1-21} enhanced its antagonistic effect because Tat-PTD contains an arginine-rich motif. These results indicate that the secondary structure and/or arginine content of peptides may be important for CXCR4 antagonism.

Since Rex_{1-21} accumulated in the nucleoli and Rex binds to the stem-loop III/IV/V region of the RRE, which is different from the recognition site of Rev (stem-loop IIB) (Ahmed et al., 1990; Kjems et al., 1992), Rex_{1-21}-PTD probably inhibited the production of viral p24 by interfering with an event after the Rev-stem-loop IIB interaction, possibly Rev oligomerization. It is possible that the increased size of Rex_{1-21}-PTD over Rex_{1-21} results somehow to increased steric hindrance that prevents REV oligomerization. It is also possible that the increased size of Rex_{1-21}-PTD over Rex_{1-21}- confers higher stability to the secondary structure of the peptide for binding to the RRE or competing with the Rev function in Rex_{1-21}. Binding of Rex_{1-21}-PTD to the stem-loop III/IV/V region, which is different from the binding of Rev (Ahmed et al., 1990), also inhibited p24 production, indicating that not only stem-loop IIB but also the whole RRE structure may represent potential drug targets. Moreover, it provides opportunities for combination therapies of peptides that target different domains of RRE.

RSG-P2G4, another arginine-rich peptide which permeates the cell membrane efficiently, (Harada et al., 1997), also inhibited viral p24 production. RSG-P2G4 binds to stem-loop IIB of the RRE (Harada et al., 1997), and therefore inhibited p24 production as efficiently as the Rev peptides.

4.2. Potential of Rev antagonists as chemotherapeutic agents

In the early phase of the HIV-1 replication cycle, Tat protein promotes production early proteins such as Tat, Rev and Nef. Since Tat enhances viral transcription without controlling splicing, the early proteins accumulate in the cells. One of the early proteins, Rev, inhibits splicing of the transcripts and exports them to the cytoplasm to generate late proteins including Gag, Pol, Env and progenitor genomes, resulting in suppression of Tat and Rev expression (Felber et al., 1990; Seelamgari et al., 2004). These decreases subsequently increase Tat expression, such that Tat and Rev cooperate for efficient viral gene expression with a certain balance. This cooperation plays an important role in the generation of progeny viruses, suggesting that interference with this cooperation may be sufficient for suppression of viral replication. Limited loss of Rev function without full suppression of its activity may cause an imbalance of Tat/Rev functions, resulting in dysregulation of viral expression and the formation of incomplete viruses. Therefore, only partial inhibitory effects of Rev inhibitors, rather than the full inhibition observed for reverse transcriptase and protease inhibitors, may be sufficient for effective viral suppression. In the state of Tat dominance, infected cells will keep producing disproportionate amounts of early proteins, such as Tat, Rev and Nef. Accumulation of such proteins may be detrimental to an antigen-presenting cell, as it may result in targeting by the host immune system, and elimination of infected cells. This would be a novel strategy for eliminating HIV-infected cells using peptide-based therapies.

As with all potential anti-HIV therapeutics a concern regarding Rev inhibitors is the development of resistance. However, it should be noted that in this case there would be additional constraints that are likely to affect the barrier to resistance. Specifically, introduction of mutations into the Rev coding region also influences the Tat and/or Env sequences and possibly their functions, as both proteins are simultaneously encoded with Rev. Furthermore, it is likely that successful introduction of mutations might interfere with the balance of Rev/Tat, which would also reduce viral replication and lead to possible elimination of the infected cells by the host immune system. In the case of RRE mutations, we have clearly demonstrated that the RRE and the gp41 N-heptad repeat (N-HR), one of the key helical domains for virus fusion, are simultaneously encoded and that mutations in the N-HR influenced RRE structure clearly affect the replication kinetics of the virus (Nameki et al., 2005; Ueno et al., 2009). These observations highlight a number of difficulties that HIV-1 would have to overcome in order to develop resistance against Rev inhibitors. Even if HIV-1 does acquire resistance, this may result in deteriorating replication kinetics, since it will simultaneously alter the functions of other viral proteins, such as Tat and gp41, and the RRE. Therefore, genetic barrier for resistance against Rev inhibitors is expected to be high and Rev inhibitors may be able to sustain antiviral activity during prolonged use.

5. Conclusion

We have shown that arginine-rich peptides derived from the RNA-binding domain of HIV-1 Rev can act as dual-target inhibitors that inhibit HIV-1 entry and viral production in the early and late phases of replication. Targeting Rev for chemotherapy is a promising strategy because it is entirely distinct from current drug targets. In addition, acquisition of resistance to Rev inhibitors may be limited because the Rev and RRE encoding regions simultaneously encode Tat and/or Env. Furthermore, the Rev peptides inhibit a completely different step of HIV-1 infection, the coreceptor CXCR4, and may, therefore, exert synergistic effects. Moreover, inhibiting Rev function may induce elimination of infected cells by the host immune system, suggesting that Rev peptides may represent the first inhibitors to enhance vaccine efficacy. Taken together, the dual-target Rev peptides are attractive agents and our present observations support their development as dual-target inhibitors for the prevention of HIV-1 infection.

Acknowledgments

We appreciate Dr. Masahiko Sugita for comments on the manuscript. We thank Dr. Kazuya Shimura, Miss Keiko Kajiwara and Mr. Makoto Shirakawa for technical assistance.

This work was supported by a grant from the Ministry of Education, Culture, Sports, Science, and Technology of Japan (E.K.), a grant for the Promotion of AIDS Research from the Ministry of Health, Labor and Welfare (to E.K. and M.M.) and a grant for Research for Health Sciences Focusing on Drug Innovation from the Japan Health Sciences Foundation (to E.K. and M.M.). K.S. is supported by the 21st

Century COE program of the Ministry of Education, Culture, Sports, Science and Technology.

References

Ahmed YF, Hanly SM, Malim MH, Cullen BR, Greene WC. Structure-function analyses of the HTLV-I Rex and HIV-1 Rev RNA response elements: insights into the mechanism of Rex and Rev action. Genes Dev 1990;4:1014–22.

Arakaki R, Tamamura H, Premanathan M, Kanbara K, Ramanan S, Katsura Mochizuki K, et al. T134, a small-molecule CXCR4 inhibitor, has no cross-drug resistance with AMD3100, a CXCR4 antagonist with a different structure. J Virol 1999;73:1719–23.

Baba M, Nishimura O, Kanzaki N, Okamoto M, Sawada H, Iizawa Y, et al. A small-molecule, nonpeptide CCR5 antagonist with highly potent and selective anti-HIV-1 activity. Proc Natl Acad Sci U S A 1999;96:5698–703.

Battiste JL, Mao H, Rao NS, Tan R, Muhandiram DR, Kay LE, et al. Alpha helix-RNA major groove recognition in an HIV-1 rev peptide-RRE RNA complex. Science 1996;273:1547–51.

Bogerd HP, Huckaby GL, Ahmed YF, Hanly SM, Greene WC. The type I human T-cell leukemia virus (HTLV-I) Rex trans-activator binds directly to the HTLV-I Rex and the type 1 human immunodeficiency virus Rev RNA response elements. Proc Natl Acad Sci U S A 1991;88:5704–8.

Charpentier B, Stutz F, Rosbash M. A dynamic in vivo view of the HIV-I Rev-RRE interaction. J Mol Biol 1997;266:950–62.

Daugherty MD, D'Orso I, Frankel AD. A solution to limited genomic capacity: using adaptable binding surfaces to assemble the functional HIV Rev oligomer on RNA. Mol Cell 2008;31:824–34.

Dayton ET, Powell DM, Dayton AI. Functional analysis of CAR, the target sequence for the Rev protein of HIV-1. Science 1989;246:1625–9.

Donzella GA, Schols D, Lin SW, Este JA, Nagashima KA, Maddon PJ, et al. AMD3100, a small molecule inhibitor of HIV-1 entry via the CXCR4 co-receptor. Nat Med 1998;4:72–7.

Doranz BJ, Grovit-Ferbas K, Sharron MP, Mao SH, Goetz MB, Daar ES, et al. A small-molecule inhibitor directed against the chemokine receptor CXCR4 prevents its use as an HIV-1 coreceptor. J Exp Med 1997;186:1395–400.

Dundr M, Leno GH, Hammarskjold ML, Rekosh D, Helga-Maria C, Olson MO. The roles of nucleolar structure and function in the subcellular location of the HIV-1 Rev protein. J Cell Sci 1995;108(Pt 8):2811–23.

Este JA, Telenti A. HIV entry inhibitors. Lancet 2007;370:81–8.

Felber BK, Drysdale CM, Pavlakis GN. Feedback regulation of human immunodeficiency virus type 1 expression by the Rev protein. J Virol 1990;64:3734–41.

Felber BK, Hadzopoulou-Cladaras M, Cladaras C, Copeland T, Pavlakis GN. rev protein of human immunodeficiency virus type 1 affects the stability and transport of the viral mRNA. Proc Natl Acad Sci U S A 1989;86:1495–9.

Fischer U, Huber J, Boelens WC, Mattaj IW, Luhrmann R. The HIV-1 Rev activation domain is a nuclear export signal that accesses an export pathway used by specific cellular RNAs. Cell 1995;82:475–83.

Futaki S, Ishikawa T, Niwa M, Kitagawa K, Yagami T. Embodying a stable alpha-helical protein structure through efficient chemical ligation via thioether formation. Bioorg Med Chem 1997;5:1883–91.

Futaki S, Suzuki T, Ohashi W, Yagami T, Tanaka S, Ueda K, et al. Arginine-rich peptides. An abundant source of membrane-permeable peptides having potential as carriers for intracellular protein delivery. J Biol Chem 2001;276:5836–40.

Hammes SR, Greene WC. Multiple arginine residues within the basic domain of HTLV-I Rex are required for specific RNA binding and function. Virology 1993;193:41–9.

Harada K, Martin SS, Frankel AD. Selection of RNA-binding peptides in vivo. Nature 1996;380:175–9.

Harada K, Martin SS, Tan R, Frankel AD. Molding a peptide into an RNA site by in vivo peptide evolution. Proc Natl Acad Sci U S A 1997;94:11887–92.

Jain C, Belasco JG. Structural model for the cooperative assembly of HIV-1 Rev multimers on the RRE as deduced from analysis of assembly-defective mutants. Mol Cell 2001;7:603–14.

Jiang F, Gorin A, Hu W, Majumdar A, Baskerville S, Xu W, et al. Anchoring an extended HTLV-1 Rex peptide within an RNA major groove containing junctional base triples. Structure 1999;7:1461–72.

Kalland KH, Szilvay AM, Langhoff E, Haukenes G. Subcellular distribution of human immunodeficiency virus type 1 Rev and colocalization of Rev with RNA splicing factors in a speckled pattern in the nucleoplasm. J Virol 1994;68:1475–85.

Kjems J, Calnan BJ, Frankel AD, Sharp PA. Specific binding of a basic peptide from HIV-1 Rev. EMBO J 1992;11:1119–29.

Kodama EI, Kohgo S, Kitano K, Machida H, Gatanaga H, Shigeta S, et al. 4'-Ethynyl nucleoside analogs: potent inhibitors of multidrug-resistant human immunodeficiency virus variants in vitro. Antimicrob Agents Chemother 2001;45:1539–46.

Lalezari JP, Henry K, O'Hearn M, Montaner JS, Piliero PJ, Trottier B, et al. Enfuvirtide, an HIV-1 fusion inhibitor, for drug-resistant HIV infection in North and South America. N Engl J Med 2003;348:2175–85.

Lazzarin A, Clotet B, Cooper D, Reynes J, Arasteh K, Nelson M, et al. Efficacy of enfuvirtide in patients infected with drug-resistant HIV-1 in Europe and Australia. N Engl J Med 2003;348:2186–95.

Lin JC, Barua B, Andersen NH. The helical alanine controversy: an (Ala)6 insertion dramatically increases helicity. J Am Chem Soc 2004;126:13679–84.

Maeda K, Nakata H, Koh Y, Miyakawa T, Ogata H, Takaoka Y, et al. Spirodiketopiperazine-based CCR5 inhibitor which preserves CC-chemokine/CCR5 interactions and exerts potent activity against R5 human immunodeficiency virus type 1 in vitro. J Virol 2004;78:8654–62.

Malim MH, Bohnlein S, Hauber J, Cullen BR. Functional dissection of the HIV-1 Rev trans-activator–derivation of a trans-dominant repressor of Rev function. Cell 1989a;58:205–14.

Malim MH, Cullen BR. HIV-1 structural gene expression requires the binding of multiple Rev monomers to the viral RRE: implications for HIV-1 latency. Cell 1991;65:241–8.

Malim MH, Hauber J, Le SY, Maizel JV, Cullen BR. The HIV-1 rev trans-activator acts through a structured target sequence to activate nuclear export of unspliced viral mRNA. Nature 1989b;338:254–7.

Mann DA, Mikaelian I, Zemmel RW, Green SM, Lowe AD, Kimura T, et al. A molecular rheostat. Co-operative rev binding to stem I of the rev-response element modulates human immunodeficiency virus type-1 late gene expression. J Mol Biol 1994;241:193–207.

Marqusee S, Robbins VH, Baldwin RL. Unusually stable helix formation in short alanine-based peptides. Proc Natl Acad Sci U S A 1989;86:5286–90.

Murakami T, Zhang TY, Koyanagi Y, Tanaka Y, Kim J, Suzuki Y, et al. Inhibitory mechanism of the CXCR4 antagonist T22 against human immunodeficiency virus type 1 infection. J Virol 1999;73:7489–96.

Nagahara H, Vocero-Akbani AM, Snyder EL, Ho A, Latham DG, Lissy NA, et al. Transduction of full-length TAT fusion proteins into mammalian cells: TAT-p27Kip1 induces cell migration. Nat Med 1998;4:1449–52.

Nameki D, Kodama E, Ikeuchi M, Mabuchi N, Otaka A, Tamamura H, et al. Mutations conferring resistance to human immunodeficiency virus type 1 fusion inhibitors are restricted by gp41 and Rev-responsive element functions. J Virol 2005;79:764–70.

Olsen HS, Cochrane AW, Dillon PJ, Nalin CM, Rosen CA. Interaction of the human immunodeficiency virus type 1 Rev protein with a structured region in env mRNA is dependent on multimer formation mediated through a basic stretch of amino acids. Genes Dev 1990;4:1357–64.

Rimsky L, Hauber J, Dukovich M, Malim MH, Langlois A, Cullen BR, et al. Functional replacement of the HIV-1 rev protein by the HTLV-1 rex protein. Nature 1988;335:738–40.

Seelamgari A, Maddukuri A, Berro R, de la Fuente C, Kehn K, Deng L, et al. Role of viral regulatory and accessory proteins in HIV-1 replication. Front Biosci 2004;9:2388–413.

Siomi H, Shida H, Nam SH, Nosaka T, Maki M, Hatanaka M. Sequence requirements for nucleolar localization of human T cell leukemia virus type I pX protein, which regulates viral RNA processing. Cell 1988;55:197–209.

Stauber R, Gaitanaris GA, Pavlakis GN. Analysis of trafficking of Rev and transdominant Rev proteins in living cells using green fluorescent protein fusions: transdominant Rev blocks the export of Rev from the nucleus to the cytoplasm. Virology 1995;213:439–49.

Szilvay AM, Brokstad KA, Kopperud R, Haukenes G, Kalland KH. Nuclear export of the human immunodeficiency virus type 1 nucleocytoplasmic shuttle protein Rev is mediated by its activation domain and is blocked by transdominant negative mutants. J Virol 1995;69:3315–23.

Tan R, Chen L, Buettner JA, Hudson D, Frankel AD. RNA recognition by an isolated alpha helix. Cell 1993;73:1031–40.

Uchida H, Maeda Y, Mitsuya H. HIV-1 protease does not play a critical role in the early stages of HIV-1 infection. Antiviral Res 1997;36:107–13.

Ueno M, Kodama EN, Shimura K, Sakurai Y, Kajiwara K, Sakagami S, Oishi S, Fujii N, Matsuoka M. Synonymous mutations in stem-loop III of Rev responsive elements enhance HIV-1 replication impaired by primary mutations for resistance to enfuvirtide. Antiviral Res 2009;82:67–72.

Vodicka MA, Goh WC, Wu LI, Rogel ME, Bartz SR, Schweickart VL, Raport CJ, Emerman M. Indicator cell lines for detection of primary strains of human and simian immunodeficiency viruses. Virology 1997;233:193–8.

Zapp ML, Hope TJ, Parslow TG, Green MR. Oligomerization and RNA binding domains of the type 1 human immunodeficiency virus Rev protein: a dual function for an arginine-rich binding motif. Proc Natl Acad Sci U S A 1991;88:7734–8.

THE JOURNAL OF BIOLOGICAL CHEMISTRY VOL. 285, NO. 50, pp. 39471–39480, December 10, 2010

Resistance Profiles of Novel Electrostatically Constrained HIV-1 Fusion Inhibitors*

Received for publication, May 18, 2010, and in revised form, September 27, 2010 Published, JBC Papers in Press, October 11, 2010, DOI 10.1074/jbc.M110.145789

Kazuya Shimura[‡1], Daisuke Nameki[‡2], Keiko Kajiwara[‡], Kentaro Watanabe[§], Yasuko Sakagami[‡], Shinya Oishi[§], Nobutaka Fujii[§], Masao Matsuoka[‡], Stefan G. Sarafianos[¶], and Eiichi N. Kodama[‡‖3]

From the [‡]Laboratory of Virus Control, Institute for Virus Research, and [§]Graduate School of Pharmaceutical Science, Kyoto University, 606-8507 Kyoto, Japan, the [‖]Division of Emerging Infectious Diseases, Tohoku University School of Medicine, 980-8575 Sendai, Japan, and the [¶]Christopher S. Bond Life Sciences Center and Department of Molecular Microbiology and Immunology, University of Missouri School of Medicine, Columbia, Missouri 65211

Human immunodeficiency virus (HIV) gp41 plays a key role in viral fusion; the N- and C-terminal heptad repeats (N-HR and C-HR) of gp41 form a stable 6-helical conformation for fusion. Therefore, HR-derived peptides, such as enfuvirtide (T-20), inhibit HIV-1 fusion by acting as decoys, and have been used for the treatment of HIV-1 infection. However, the efficacy of T-20 is attenuated by resistance mutations in gp41, including V38A and N43D. To suppress the resistant variants, we previously developed electrostatically constrained peptides, SC34 and SC34EK, and showed that both exhibited potent anti-HIV-1 activity against wild-type and T-20-resistant variants. In this study, to clarify the resistance mechanism to this next generation of fusion inhibitors, we selected variants with resistance to SC34 and SC34EK *in vitro*. The resistant variants had multiple mutations in gp41. All of these mutations individually caused less than 6-fold resistance to SC34 and SC34EK, indicating that there is a significant genetic barrier for high-level resistance. Cross-resistance to SC34 and SC34EK was reduced by a simple difference in the polarity of two intramolecular electrostatic pairs. Furthermore, the selected mutations enhanced the physicochemical interactions with N-HR variants and restored activities of the parental peptide, C34, even to resistant variants. These results demonstrate that our approach of designing gp41-binding inhibitors using electrostatic constraints and information derived from resistance studies produces inhibitors with enhanced activity, high genetic barrier, and distinct resistance profile from T-20 and other inhibitors. Hence, this is a promising approach for the design of future generation peptide fusion inhibitors.

The *env* gene of human immunodeficiency virus (HIV) encodes two glycoproteins, gp120 and gp41, that form a stable trimeric complex consisting of three heterodimers to constitute a functional envelope (1). Entry of HIV into target cells is initiated by the interaction of gp120 with the receptor, CD4, and then with co-receptors CCR5 or CXCR4, which are expressed on the target cell surface (2). After receptor binding, a conformational change in gp41 is induced, triggering the exposure of the N-terminal heptad repeat (N-HR)[4] by stretching the folded gp41, enabling a hydrophobic fusion domain located at the N terminus to be inserted into the target cell membrane (3). Subsequently, the N-HR folds into its counterpart, the C-terminal heptad repeat (C-HR), and together they form a hairpin-like structure of antiparallel helices (6-helix bundle) bringing together and facilitating the fusion of the viral and cellular membranes (4, 5).

Based on the nature of the mechanism of HIV fusion, peptides corresponding to N-HR or C-HR of HIV fusion acted as decoys and interfered with formation of the 6-helix bundle (6, 7). Indeed, a C-HR-derived peptide, enfuvirtide (T-20), suppresses HIV-1 replication, and has been widely used for treatment of HIV-1 infection (8, 9). However, during long-term therapy, T-20-resistant variants emerge among patients treated with T-20-containing regimens (10, 11). To suppress replication of such variants and obtain sustained efficacy, the next generation of fusion inhibitors is urgently needed.

Recently, a number of next generation peptide fusion inhibitors has been reported. These inhibitors include tifuvirtide (T-1249) (12), T-2410 (13), and sifuvirtide (14), which are able to suppress T-20-resistant variants. We have developed electrostatically constrained fusion inhibitors, SC34 and SC34EK, which inhibit replication of T-20-resistant HIV-1 (15). SC34 was designed to be more soluble and have enhanced α-helicity, by engineering electrostatic interactions between glutamic acid and lysine substitutions at i and $i+4$ positions in the solvent-interacting site (EK motif) (16) of the parental C-HR-derived C34 peptide (Fig. 1) (17). SC34EK, which has unidirectional EK motifs, demonstrated a 5-fold enhanced activity compared with the original C34 (15, 17). We demonstrated that the α-helical structure was stabilized by electrostatic in-

* This work was supported, in whole or in part, by National Institutes of Health Grants AI076119, AI074389, and AI079801 (to S. G. S.), in part by a grant for Promotion of AIDS Research from the Ministry of Health and Welfare of Japan (to E. N. K. and M. M.), a grant for Research on Health Science Focusing on Drug Innovation from the Japan Health Science Foundation (to E. N. K. and M. M.), and a grant from the Ministry of Education, Culture, Sports, Science and Technology of Japan (to E. N. K.).

[1] Supported by a fellowship from the Japan Health Science Foundation. To whom correspondence may be addressed: 53 Shogoin Kawahara-cho, Sakyo-ku, Kyoto 606-8507, Japan. Tel.: 81-75-751-4048; Fax: 81-75-751-4049; E-mail: kshimura@virus.kyoto-u.ac.jp.

[2] Present address: Taiho Pharmaceutical Co., Ltd., Hanno, Japan.

[3] To whom correspondence may be addressed: Division of Emerging Infectious Diseases, Tohoku University School of Medicine, Bldg. 1, Rm. 515, 2-1 Seiryocho, Aoba-ku, Sendai 980-8575, Japan. Tel.: 81-22-717-7199; Fax: 81-22-717-8221; E-mail: kodama515@med.tohoku.ac.jp.

[4] The abbreviations used are: N-HR, N-terminal heptad repeat; C-HR, C-terminal heptad repeat; MAGI, multinuclear activation of a galactosidase indicator.

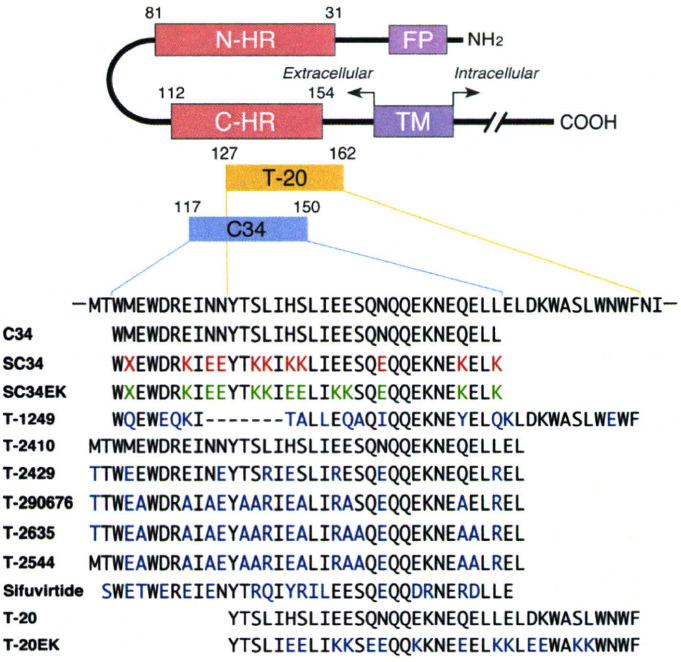

FIGURE 1. **Peptide sequences of gp41-derived fusion inhibitors.** C-HR-derived fusion inhibitors are shown with the functional domains of HIV-1 gp41. The residue numbers of each peptide correspond to their positions in gp41 of HIV-1_{NL4-3}. *FP*, fusion peptide; *TM*, transmembrane domain; *X*, norleucine (Nle); −, deleted amino acid.

teractions of the EK motif with specific residues on the target peptide, providing high selectivity (15).

In addition to engineering stabilizing electrostatic interactions we have also established a second strategy to design improved peptide fusion inhibitors. This strategy is based on the introduction of resistance mutations into the sequence of the original peptide inhibitor. These new changes enhance the antiviral potency against resistant variants. Hence, T-20 with a S138A substitution (T-20_{S138A}), one of the secondary resistance mutations observed in patients that fail to respond to T-20, regained anti-HIV-1 activity against T-20-resistant variants (18). X-ray crystallographic and circular dichroism (CD) analyses revealed that the S138A substitution contributed to stability of the N-HR·C-HR complex (19). Similar results were observed for C34 with N126K ($C34_{N126K}$), also secondary mutations for T-20-resistant variants *in vivo* (20, 21) and C34-resistant variants *in vitro* (18). Therefore, the novel strategy to design inhibitor peptides utilizing resistance mutations has resulted in antivirals that can suppress variants resistant to the parental peptides.

In this study, to determine the mechanism of resistance and the effect of escape mutations on the potency of the next generation fusion inhibitors, we induced resistant variants to SC34 and SC34EK *in vitro*. Our results demonstrate that peptides that are designed to have specific electrostatic constraints and include changes that are based on resistance information have significantly improved properties in terms of potency and cross-resistance.

EXPERIMENTAL PROCEDURES

Antiviral Agents—Peptide fusion inhibitors (Fig. 1) were synthesized based on a previous report (17). 2′,3′-Dideoxycytidine was purchased from Sigma.

Cells and Viruses—MT-2 and 293T cells were grown in RPMI1640 medium and Dulbecco's modified Eagle's medium (DMEM), respectively. These media were supplemented with 10% fetal calf serum (FCS), 2 mM L-glutamine, 100 units/ml of penicillin, and 50 μg/ml of streptomycin. HeLa-CD4/CCR5-LTR/β-gal cells (22) (provided by Dr. J. Overbaugh through the NIH AIDS Research and Reference Reagent Program, Division of AIDS, NIAID) were maintained in DMEM supplemented with 10% FCS, 200 μg/ml of hygromycin B, 10 μg/ml of puromycin, and 200 μg/ml of geneticin.

An HIV-1 molecular clone, pNL4-3 (23), was employed as a wild-type HIV-1 (HIV-1_{NL4-3}), and used for the construction of various gp41-recombinant viruses as described previously (15, 18, 24, 25). The viruses were harvested from the supernatant of transfected 293T cells and stored at −80 °C.

Determination of Drug Susceptibility—Anti-HIV activity of inhibitors was determined using multinuclear activation of a galactosidase indicator (MAGI) assay as described previously (15, 18, 24–26). Inhibitory activity was presented as the concentration required for 50% inhibition (EC_{50}).

Dose Escalating Induction of Resistant Variants to SC34 or SC34EK—MT-2 cells were initially infected with HIV-1_{NL4-3} in the presence of 0.1 nM SC34 or 0.15 nM SC34EK. Infected cells were incubated at 37 °C until a cytopathic effect was observed. When an extensive cytopathic effect was observed, culture supernatant was harvested and used for the next round of infection on fresh MT-2 cells in the presence of a 2-fold increased concentration of inhibitors as shown in Fig. 2. At the indicated passages, proviral DNA was extracted from infected cells and the mutations were identified by direct sequencing. These selections with dose escalations were performed in a single HIV-1 selection culture. To avoid selection of a minor population for drug resistance, in each passage, we propagated the virus after an extensive cytopathic effect was observed.

Replication Kinetics of Env-recombinant Viruses—MT-2 cells (10^5 cells/3 ml) were infected with each env-recombinant HIV-1 clone (500 MAGI units) for 4 h. The infected cells were extensively washed and cultured in 4 ml in 6-well plates. The culture supernatants were harvested periodically and production of progeny viruses was monitored by the MAGI assay.

Circular Dichroism (CD) Spectroscopic Analysis—CD analysis was performed as described previously (15, 18, 27), with some modifications. In brief, spectra of a complex of N-HR and C-HR peptides (each 10 μM) or an N-HR peptide alone (10 μM) in 5 mM HEPES buffer (pH 7.2) were collected using a J-710 CD spectrometer (Jasco, Tokyo, Japan) equipped with a thermoelectric temperature controller. The thermal stability was measured as the change of CD signal at 222 nm. The temperature that resulted in 50% unfolding (melting temperature, T_m) of each complex was determined.

Statistical Analysis—Pearson correlation analysis of relationships between T_m values of each N-HR·C-HR complex determined in the CD analysis, and the EC_{50} values of inhibitors determined by MAGI assay, was performed using GraphPad Prism 4 software (GraphPad Software Inc., San Diego, CA). *p* values less than 0.05 were considered statistically significant.

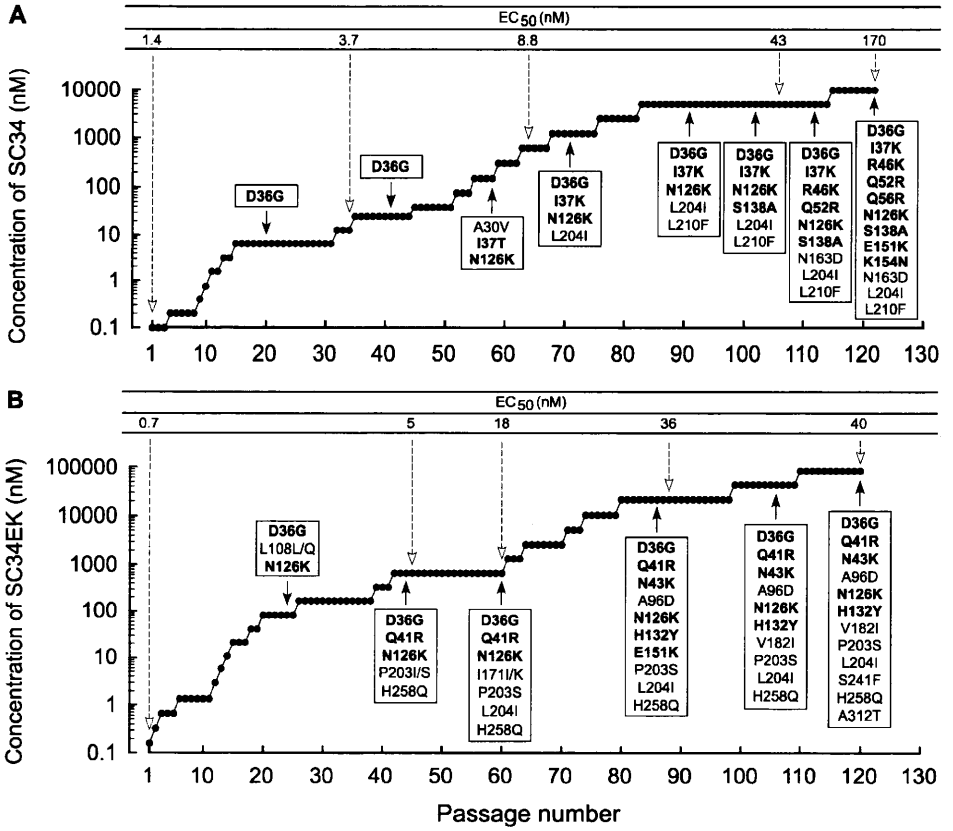

FIGURE 2. **Induction of SC34- and SC34EK-resistant HIV-1.** HIV-1_{NL4-3} was passaged in the presence of increasing concentrations of the inhibitors in MT-2 cells. The dose escalating selections were carried out for a total of 122 passages with SC34 concentrations ranging from 0.1 nM to 9.8 μM (*A*), and for 120 passages with SC34EK concentrations ranging from 0.15 nM to 80 μM (*B*). At the indicated passage number (*black arrowheads* with *solid line*), proviral DNA was extracted from infected cells, and gp41- and gp120-coding regions were sequenced. At the final passage (P-122 for SC34 and P-120 for SC34EK), the following gp120 mutations were identified; K107K/Q (mixture of K and Q), S134N, S136G, and F147L in the case of SC34, and V37A, V59I, S100K, S115N, R138S, D139N, and A310T in the case of SC34EK. Amino acids shown in *bold* are located within the N-HR (31–81) or C-HR (112–154) in the gp41. The EC_{50} values of HIV-1 variants (heterogeneous pool) at the indicated passage number (*white arrowheads* with *dashed line*) were determined using the MAGI assay.

RESULTS

Selection of SC34-resistant HIV-1 in Vitro—To determine the resistance profile of SC34, SC34-resistant variants were selected by a dose-escalating method and susceptibility of the obtained variants was determined by the MAGI assay. Selection of resistant HIV-1_{NL4-3} was initially started in the presence of 0.1 nM SC34 (Fig. 2*A*). At passage 20 (P-20), where the concentration of SC34 was 6.4 nM, substitution of aspartic acid to glycine at position 36 in the gp41 coding region (D36G) was observed. At P-58, although the D36G substitution transiently reverted to the original amino acid, a set of mutations, A30V, I37T, and N126K, which also emerged during the induction of resistance to C34 (24), was introduced. At P-71, D36G was again observed, and simultaneously, L204I was introduced, whereas A30V disappeared. L210F and S138A were newly introduced at P-91 and P-102, respectively. The EC_{50} of SC34 to the P-106 variant increased to 43 nM. At P-112, further substitutions, R46K, Q52R, and N163D, were added. The amino acid at position 163 was predominantly aspartic acid among many HIV-1 strains (28). Therefore, the N163D change was considered to be a polymorphism. At the final passage, P-122, Q56R, E151K, and K154N were further introduced, and the EC_{50} for SC34 reached 170 nM. In addition to the mutations introduced in the gp41, some mutations were also identified in gp120 at P-122 (K107K/Q (a mixture of Lys and Gln), S134N, S136G, and F147L.

Selection of SC34EK-resistant HIV-1 in Vitro—Induction of SC34EK resistance was also performed, except that the initial concentration of SC34EK was 0.15 nM (Fig. 2*B*). At P-24, two substitutions, D36G and N126K, were observed in the gp41. A transient partial substitution at Leu^{108} was observed as a mixture of leucine and glutamine (L108L/Q), but disappeared at later passages. At P-44, Q41R, P203I/S, and H258Q were added. Heterogeneous P203I/S at P-44 was transient, and was predominantly substituted by P203S at P-60. The EC_{50} of SC34EK to P-45 variants was 5 nM. At P-60, I171I/K and L204I were added, and the EC_{50} increased to 18 nM. At P-86, four further substitutions, N43K, A96D, H132Y, and E151K, were newly introduced. The EC_{50} of SC34EK to the P-88 variant increased to 36 nM. Further substitutions, V182I and S241F/A312T, emerged at P-106 and P-120, respectively. The EC_{50} of SC34EK for the P-120 variant ultimately reached 40 nM. H132Y and V182I observed at later passages were considered gp41 polymorphisms, because these were predominantly observed in non-treated clinical isolates (28). Mutations introduced in the gp120 at the final P-120 were V37A, V59I, S100K, S115N, R138S, D139N, and A310T.

TABLE 1

Susceptibility of SC34-selected mutation-introduced env-recombinant viruses to fusion inhibitors

Anti-HIV activity was determined using MAGI assay. Data are shown as mean ± S.D. obtained from at least three independent experiments, and resistance (*n*-fold of the EC_{50}) of recombinant viruses, compared to that of parental HIV-1_{NL4-3}, is shown in parentheses.

Mutation(s)	EC_{50} (nM)				
	ddC	T-20	C34	SC34	SC34EK
HIV-1_{NL4-3}[a]	430 ± 121	20 ± 3	3.3 ± 0.6	1.4 ± 0.3	0.7 ± 0.4
gp41					
A30V	213 ± 40 (0.5)	6.4 ± 2.2 (0.3)	7.2 ± 1.6 (2.2)	0.5 ± 0.2 (0.4)	0.8 ± 0.2 (1.1)
D36G	392 ± 93 (0.9)	1.0 ± 0.1 (0.05)	8.1 ± 3.4 (2.5)	0.6 ± 0.2 (0.4)	0.7 ± 0.2 (1.0)
I37K	287 ± 92 (0.7)	2,453 ± 873 (123)	23 ± 3 (7.0)	4.9 ± 0.6 (3.5)	1.0 ± 0.2 (1.4)
I37T	289 ± 30 (0.7)	166 ± 40 (8.3)	20 ± 5 (6.1)	2.3 ± 0.8 (1.6)	0.5 ± 0.1 (0.7)
R46K	572 ± 162 (1.3)	ND[b]	1.3 ± 0.4 (0.4)	0.6 ± 0.1 (0.4)	1.9 ± 0.2 (2.7)
Q52R	415 ± 29 (1.0)	ND	2.9 ± 0.8 (0.9)	1.6 ± 0.5 (1.1)	1.5 ± 0.2 (2.1)
Q56R	300 ± 58 (0.7)	ND	28 ± 6 (8.5)	4.1 ± 1.0 (2.9)	1.0 ± 0.2 (1.4)
N126K	256 ± 18 (0.6)	27 ± 5 (1.4)	8.0 ± 2.9 (2.4)	1.3 ± 0.4 (0.9)	0.4 ± 0.1 (0.6)
S138A	210 ± 64 (0.5)	ND	4.0 ± 0.8 (1.2)	2.3 ± 0.8 (1.6)	0.8 ± 0.2 (1.1)
E151K	277 ± 16 (0.6)	ND	2.3 ± 0.6 (0.7)	1.1 ± 0.02 (0.8)	1.4 ± 0.4 (2.0)
K154N	529 ± 160 (1.2)	ND	2.1 ± 1.7 (0.6)	1.4 ± 0.5 (1.0)	0.4 ± 0.2 (0.6)
N163D	348 ± 33 (0.8)	ND	0.5 ± 0.1 (0.2)	2.5 ± 0.8 (1.8)	0.9 ± 0.7 (1.3)
L204I	226 ± 12 (0.5)	13 ± 4 (0.7)	3.9 ± 0.1 (1.2)	1.5 ± 0.3 (1.1)	0.6 ± 0.1 (0.9)
L210F	556 ± 162 (1.3)	ND	4.1 ± 1.7 (1.2)	0.6 ± 0.1 (0.4)	0.4 ± 0.04 (0.6)
SC34(P-122)gp41[c]	329 ± 33 (0.8)	1,727 ± 255 (86)	24 ± 4 (7.3)	2,189 ± 287 (1,564)	23 ± 1 (33)
gp120					
SC34(P-122)gp120[d]	339 ± 95 (0.8)	45 ± 2 (2.3)	0.8 ± 0.3 (0.2)	0.2 ± 0.03 (0.1)	0.2 ± 0.05 (0.3)
gp160					
SC34(P122)gp160[e]	542 ± 68 (1.3)	>5,000 (>250)	>1,000 (>303)	2,827 ± 439 (2,019)	33 ± 4 (47)

[a] HIV-1_{NL4-3} was used as wild-type virus.
[b] ND, not determined.
[c] HIV-$1_{SC34(P-122)gp41}$ contains D36G/I37K/R46K/Q52R/Q56R/N126K/S138A/E151K/K154N/N163D/L204I/L210F mutations in gp41 coding region.
[d] HIV-$1_{SC34(P-122)gp120}$ contains K107Q/S134N/S136G/F147L mutations in gp120 coding region.
[e] HIV-$1_{SC34(P-122)gp160}$ contains K107Q/S134N/S136G/F147L and D36G/I37K/R46K/Q52R/Q56R/N126K/S138A/E151K/K154N/N163D/L204I/L210F mutations in gp120 and gp41 coding regions, respectively.

Acquisition of resistance to SC34EK seems to be faster than that to SC34 (Fig. 2). However, actual EC_{50} values for SC34 and SC34EK remain just 8.5- and 2-fold of that of T-20, respectively.

Phenotypic Analysis of gp41-, gp120-, and gp160-recombinant HIV-1—To determine which mutations contributed to inhibitor resistance we constructed gp41 recombinant HIV-1s containing each of the mutations that emerged during resistant variant selection. Changes of susceptibility were determined by the MAGI assay (Tables 1 and 2). During T-20 therapy, HIV-1 acquired T-20 resistance mutations, especially in amino acids at positions 36–45 (DIVQQQNNLL in the NL4–3 sequence) of gp41 N-HR, where it interacts with C-HR, mainly contributing to the resistance (29–32). In our selections using SC34 and SC34EK, several mutations were also located within this region, and some conferred T-20 resistance to various extents (123- and 14-fold by I37K and N43K, respectively). I37K was slightly resistant to SC34 (3.5-fold). Ile^{37} was initially substituted with threonine (I37T) at P-58, and later converted to lysine (I37K) at P-71, moderately reducing the susceptibility to SC34 (from 1.6- to 3.5-fold). Other substitutions had little influence on the susceptibility to SC34 (0.4–2.9-fold decreases). However, HIV-$1_{SC34(P-122)gp41}$, which contains multiple substitutions, D36G/I37K/R46K/Q52R/Q56R/N126K/S138A/E151K/K154N/N163D/L204I/L210F, showed high resistance to SC34 (1564-fold) and T-20 (86-fold), but mild and moderate resistance to C34 (7.3-fold) and SC34EK (33-fold), respectively.

The A96D mutation observed in SC34EK selection conferred high resistance to T-20 (more than 50-fold), but only weak resistance to SC34EK (6.3-fold) (Table 2). Ala^{96} is located between two HRs, termed a loop or hinge region, and so far, there are no clinical reports that A96D is involved in T-20 resistance during antiviral therapy. It is likely that the A96D substitution that introduces a larger polar residue at position 96 induces structural changes to gp41, resulting in reduced T-20 interaction. However, the exact effects of the A96D mutation on the resistance remain unclear. An N43K mutation, which is observed in T-20-treated HIV-1-infected patients, decreased susceptibility to C34 (55-fold), whereas it had little effect on the susceptibility to SC34 (1.9-fold) and SC34EK (3.3-fold). An H132Y substitution also conferred mild and moderate resistance to SC34EK and T-20 (4.9- and 18-fold, respectively), but not to C34 and SC34. Substitutions other than A96D and H132Y had little influence on the susceptibility to SC34EK (range of fold-decrease in resistance was 0.6–3.3). However, HIV-$1_{SC34EK(P-120)gp41}$, which contains multiple substitutions, D36G/Q41R/N43K/A96D/N126K/H132Y/V182I/P203S/L204I/S241F/H258Q/A312T, again conferred high resistance to SC34EK (107-fold), but moderate resistance to both C34 (21-fold) and SC34 (14-fold).

The vast majority of HIV-1 strains carry a glycine at position 36 (G36), but in rare cases, NL4-3 harbors aspartic acid (Asp^{36}) (28). We recently observed that D36G is selected during passages even in the absence of peptide inhibitors,[5] indicating that D36G is an HIV-1_{NL4-3}-specific substitution.

We also evaluated the effect of mutations in the gp120 on drug susceptibility. The two clones, HIV-$1_{SC34(P-122)gp120}$ and HIV-$1_{SC34EK(P-120)gp120}$ containing K107Q/S134N/S136G/F147L and V37A/V59I/S100K/S115N/R138S/D139N/A310T mutations, respectively, showed no significant resistance to

[5] K. Shimura, D. Nameki, K. Kajiwara, K. Watanabe, Y. Sakagami, S. Oishi, N. Fujii, M. Matsuoka, S. G. Sarafianos, and E. Kodama, unpublished data.

TABLE 2

Susceptibility of SC34EK-selected mutation-introduced env-recombinant viruses to fusion inhibitors

Anti-HIV activity was determined using MAGI assay. Data are shown as mean ± S.D. obtained from at least three independent experiments, and resistance (*n*-fold of the EC_{50}) of recombinant viruses, compared to that of parental HIV-1_{NL4-3}, is shown in parentheses.

Mutation(s)	EC_{50} (nM)				
	ddC	T-20	C34	SC34	SC34EK
HIV-1_{NL4-3}[a]	430 ± 121	20 ± 3	3.3 ± 0.6	1.4 ± 0.3	0.7 ± 0.4
gp41					
D36G	392 ± 93 (0.9)	1.0 ± 0.1 (0.05)	8.1 ± 3.4 (2.5)	0.6 ± 0.2 (0.4)	0.7 ± 0.2 (1.0)
Q41R	259 ± 19 (0.6)	ND[b]	125 ± 50 (38)	5.3 ± 0.4 (3.8)	2.3 ± 0.6 (3.3)
N43K	220 ± 5.0 (0.5)	278 ± 24 (14)	180 ± 54 (55)	2.7 ± 0.6 (1.9)	2.3 ± 0.8 (3.3)
A96D	255 ± 13 (0.6)	>1,000 (>50)	12 ± 1 (3.6)	2.8 ± 1.2 (2.0)	4.4 ± 0.9 (6.3)
N126K	256 ± 18 (0.6)	27 ± 5 (1.4)	8.0 ± 2.9 (2.4)	1.3 ± 0.4 (0.9)	0.4 ± 0.1 (0.6)
H132Y	394 ± 83 (0.9)	363 ± 70 (18)	3.6 ± 1.4 (1.1)	2.7 ± 1.3 (1.9)	3.4 ± 0.4 (4.9)
E151K	277 ± 16 (0.6)	ND	2.3 ± 0.6 (0.7)	1.1 ± 0.02 (0.8)	1.4 ± 0.4 (2.0)
V182I	686 ± 181 (1.6)	26 ± 8 (1.3)	4.5 ± 1.2 (1.4)	1.3 ± 0.3 (0.9)	0.7 ± 0.2 (1.0)
P203S	ND	ND	ND	ND	ND
L204I	226 ± 12 (0.5)	13 ± 4 (0.7)	3.9 ± 0.1 (1.2)	1.5 ± 0.3 (1.1)	0.6 ± 0.1 (0.9)
P203S/L204I	646 ± 208 (1.5)	23 ± 5 (1.2)	3.5 ± 0.1 (1.1)	1.6 ± 0.2 (1.1)	1.5 ± 0.2 (2.1)
S241F	420 ± 75 (1.0)	20 ± 3 (1.0)	6.3 ± 0.2 (1.9)	1.6 ± 0.3 (1.1)	0.6 ± 0.1 (0.9)
H258Q	381 ± 25 (0.9)	54 ± 19 (2.7)	13 ± 3 (3.9)	1.8 ± 0.4 (1.3)	0.7 ± 0.4 (1.0)
A312T	ND	ND	ND	ND	ND
H258Q/A312T	633 ± 140 (1.5)	28 ± 5 (1.4)	6.0 ± 0.7 (1.8)	1.3 ± 0.2 (0.9)	0.7 ± 0.2 (1.0)
SC34EK(P-120)gp41[c]	536 ± 20 (1.2)	112 ± 38 (5.6)	70 ± 9 (21)	20 ± 1 (14)	75 ± 8 (107)
gp120					
SC34EK(P-120)gp120[d]	399 ± 85 (0.9)	70 ± 16 (3.5)	1.4 ± 0.4 (0.4)	0.2 ± 0.03 (0.1)	0.3 ± 0.1 (0.4)
gp160					
SC34EK(P-120)gp160[e]	344 ± 42 (0.8)	435 ± 139 (22)	378 ± 133 (115)	5.2 ± 0.5 (3.7)	72 ± 18 (103)

[a] HIV-1_{NL4-3} was used as wild-type virus.
[b] ND, not determined.
[c] HIV-$1_{SC34EK(P-120)gp41}$ contains D36G/Q41R/N43K/A96D/N126K/H132Y/V182I/P203S/L204I/S241F/H258Q/A312T mutations in gp41-coding region.
[d] HIV-$1_{SC34EK(P-120)gp120}$ contains V37A/V59I/S100K/S115N/R138S/D139N/A310T mutations in gp120-coding region.
[e] HIV-$1_{SC34EK(P-120)gp160}$ contains V37A/V59I/S100K/S115N/R138S/D139N/A310T and D36G/Q41R/N43K/A96D/N126K/H132Y/V182I/P203S/L204I/S241F/H258Q/A312T mutations in gp120- and gp41-coding regions, respectively.

T-20, C34, SC34, and SC34EK. Instead, they exhibited hypersensitivity to SC34, SC34EK, and C34, and only moderate resistance to T-20 (less than 4-fold). Moreover, the gp120 mutations barely enhanced resistance conferred by the mutations gp41 (1.3- and 1.0-fold resistance to SC34 and SC34EK, respectively). Of note, when the SC34-selected mutations in gp41 and gp120 were both present in gp160, we observed significant increases in resistance to T-20 (from 86- to >250-fold) and C34 (from 7.3- to >303-fold). Similarly, when the SC34EK-selected mutations in gp41 and gp120 were present at the same time, we observed an increase in resistance to T-20 from 5.6- to 22-fold and to C34 from 21- to 115-fold. These results indicate that resistance to SC34 and SC34EK require accumulation of multiple mutations, rather than certain primary mutation(s) in the gp41, which is distinct from the mechanism of resistance to T-20 and C34.

Replication Kinetics of Env-recombinant HIV-1—The effects of SC34- and SC34EK-selected mutations in gp120 and gp41 on HIV-1 replication kinetics were assessed by measuring production levels of infectious virions in the culture supernatant by MAGI assay. Replication kinetics of clones containing SC34-selected mutations were little and moderately reduced by mutations in gp120 and gp41, respectively (Fig. 3). The reduced replication capacity observed in HIV-$1_{SC34(P-122)gp41}$ was partially restored by mutations in the gp120 (HIV-$1_{SC34(P-122)gp160}$). Similarly, SC34EK-selected mutations in gp120 partially improved the replication capacity of HIV-$1_{SC34EK(P-120)gp41}$, which was severely impaired by mutations in gp41. Taken together, these results and phenotypic analyses (Tables 1 and 2) indicate that SC34- and SC34EK-selected mutations in the gp41, not in the gp120, are mainly involved in resistance to SC34 and SC34EK with replication cost, whereas mutations in the gp120 partially restore the replication capacity through secondary mutations.

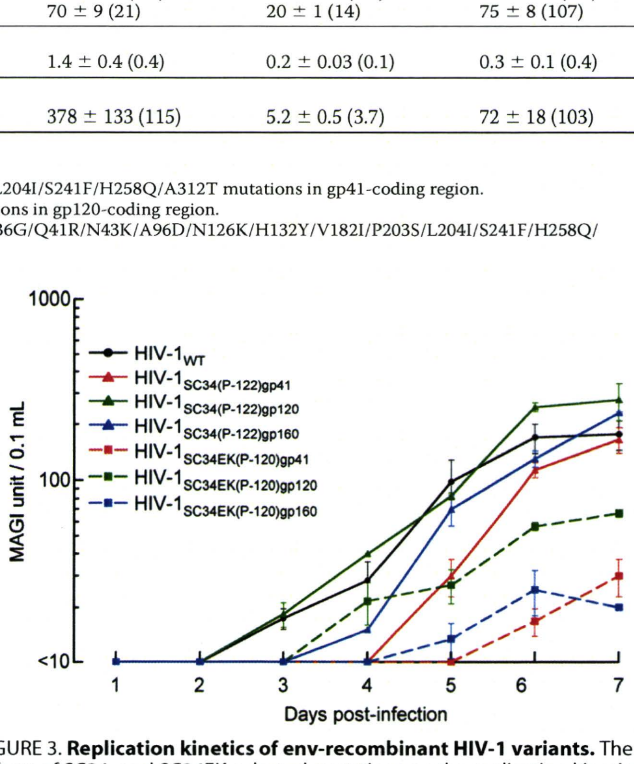

FIGURE 3. **Replication kinetics of env-recombinant HIV-1 variants.** The effects of SC34- and SC34EK-selected mutations on the replication kinetics were analyzed. MT-2 cells were infected with each env-recombinant HIV-1 variant at 500 MAGI units. After a 4-h incubation, the infected cells were washed and cultured for 7 days. The culture supernatants were harvested every 24 h and production of progeny viruses was monitored by MAGI assay. HIV-1_{NL4-3} was used as wild-type strain (HIV-1_{WT}). The presented data are mean ± S.D. of MAGI units obtained from 0.1 ml of culture supernatants. Results shown are representative of three independent experiments each using two independent clones. *Error bars* on each point represent the S.D. of the mean.

Effect of Mutations on the Stability of the α-Helical Bundle Formation—To elucidate the impact of SC34- and SC34EK-selected mutations introduced in N-HR and C-HR on the stability of complex formation between N-HR and C-HR, CD analysis was performed. The N36 peptide was used as a wild-

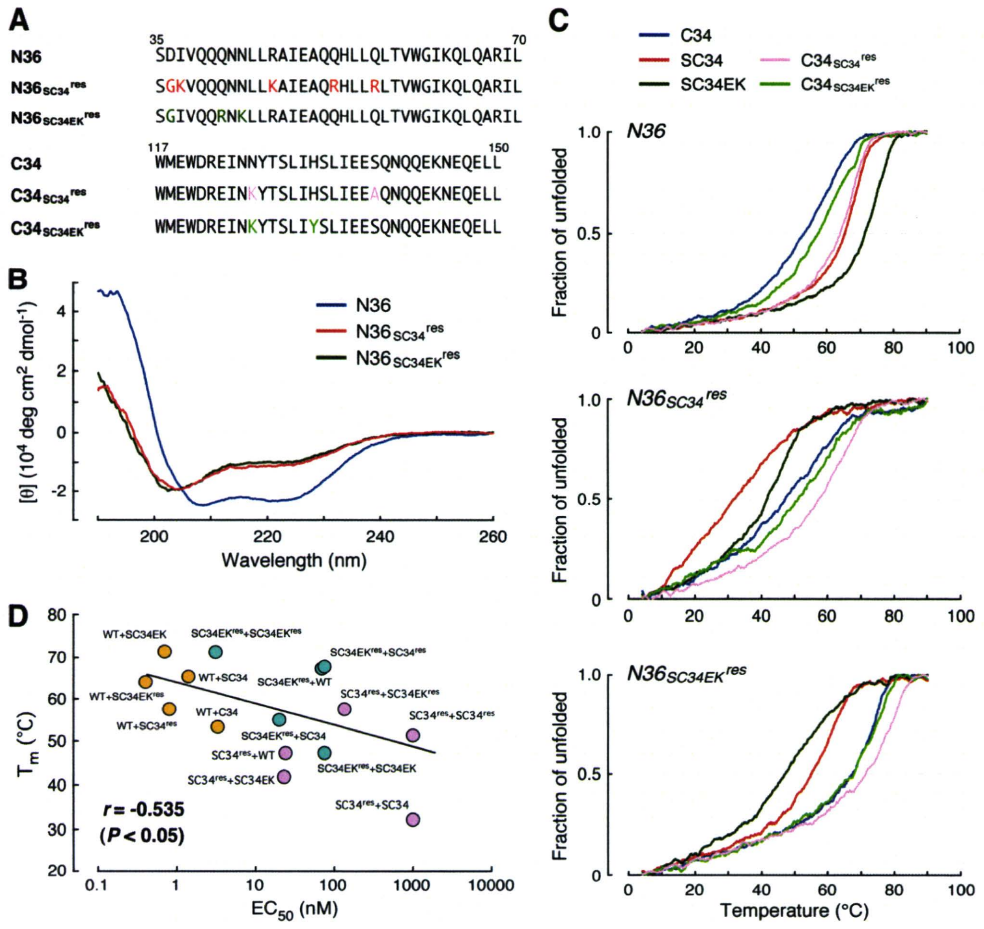

FIGURE 4. **CD analysis of physicochemical properties of fusion inhibitors.** *A*, modified peptides with mutations selected by SC34 or SC34EK were chemically synthesized. The mutations observed in the N-HR and C-HR were introduced into the original sequences of N36 and C34, respectively. Substituted amino acids are shown in *color*. *B*, CD spectra change of N-HR peptide alone. Original N36, SC34-selected mutation-introduced N36 ($N36_{SC34}^{res}$), and SC34EK-selected mutation-introduced N36 ($N36_{SC34EK}^{res}$) were separately prepared and their α-helicities, defined as molar ellipticity (θ), were examined. *C*, thermal midpoint analysis was measured at 222 nm for N-HR (N36) and C-HR (C34) peptide complexes. Equimolar amounts of N-HR and C-HR were mixed and the thermal-induced unfolding transition was measured. Original N36 (*top*), $N36_{SC34}^{res}$ (*middle*), and $N36_{SC34EK}^{res}$ (*bottom*) were used as N-HRs. C34, SC34, SC34EK, and mutation-introduced C34 ($C34_{SC34}^{res}$ and $C34_{SC34EK}^{res}$) are indicated in *color*. *D*, correlation between T_m values of each N-HR·C-HR complex determined in *C* and antiviral activity of C-HR peptides (EC_{50} values determined by MAGI assay). Combination of N-HR and C-HR peptide pairs is indicated as "N-HR + C-HR" in each plot. *Orange*, original N36; *pink*, $N36_{SC34}^{res}$; *blue*, $N36_{SC34EK}^{res}$. Pearson correlation coefficient (*r*) and its *p* value were calculated.

type N-HR. The mutant peptides, $N36_{SC34}^{res}$ and $N36_{SC34EK}^{res}$, harboring SC34-selected mutations (D36G/I37K/R46K/Q52R/Q56R) and SC34EK-selected mutations (D36G/Q41R/N43K) were prepared through chemical synthesis (Fig. 4*A*). $C34_{SC34}^{res}$ and $C34_{SC34EK}^{res}$ that contain N126K/S138A and N126K/H132Y substitutions, respectively, were also synthesized.

First, we compared the α-helicity of each N-HR peptide alone. In contrast to native N36, no typical features of α-helices were observed in either $N36_{SC34}^{res}$ or $N36_{SC34EK}^{res}$ (Fig. 4*B*). Additionally, few significant temperature-dependent changes of spectra were observed in both $N36_{SC34}^{res}$ and $N36_{SC34EK}^{res}$ over a broad range of temperatures compared with N36 (data not shown). This indicated that both inhibitors resulted in the selection of N-HR mutations that decreased the helical content and only the original N36 folded into an intramolecular coiled-coil form and behaved as an α-helix.

Thermal stability of the complex formed between N-HR and C-HR was investigated. The midpoint of the thermal unfolding transition (T_m) of N36·C34 was 53.3 °C, whereas N36·SC34 and N36·SC34EK formed more stable complexes (T_m values of 65.4 °C for N36·SC34 and 71.4 °C for N36·SC34EK; Fig. 4*C*). The resistance mutations in the C-HR enhanced binding stability; T_m of 64.1 °C for N36·$C34_{SC34}^{res}$ and 57.5 °C for N36·$C34_{SC34EK}^{res}$. C34, $C34_{SC34}^{res}$, and $C34_{SC34EK}^{res}$ maintained binding capacity to both $N36_{SC34}^{res}$ and $N36_{SC34EK}^{res}$ (Fig. 4*C*). SC34 and SC34EK no longer formed stable complexes with $N36_{SC34}^{res}$ and $N36_{SC34EK}^{res}$, as their T_m values were lower than C34. These results indicate that substitutions of compensatory mutations into C-HR contribute to stability enhancement. To further evaluate whether decreased susceptibility of the resistant variants to the inhibitors was caused by thermodynamic instability of the peptide bundle formation, we analyzed the relationship between the values of T_m and EC_{50}. The T_m was determined by CD analysis and found to be inversely correlated with the EC_{50} value measured in the MAGI assay (Pearson correlation analysis, $r = -0.535$, $p < 0.05$; Fig. 4*D*). Overall, these experiments demonstrate that mutations within N-HR reduce its α-helic-